Author Manuscript

Author Manuscript

Author Manuscript

Author Manuscript

HHS Public Access

Author manuscript

Cell Rep. Author manuscript; available in PMC 2021 June 09.

Published in final edited form as:

Cell Rep. 2021 April 06; 35(1): 108951. doi:10.1016/j.celrep.2021.108951.

Activity-dependent somatodendritic dopamine release in the substantia nigra autoinhibits the releasing neuron

Takuya Hikima[1], **Christian R. Lee**[1], **Paul Witkovsky**[1], **Julia Chesler**[1], **Konstantin Ichtchenko**[2], **Margaret E. Rice**[1,3,4,*]

[1]Department of Neurosurgery, New York University Grossman School of Medicine, New York, NY 10016, USA

[2]Department of Biochemistry & Molecular Pharmacology, New York University Grossman School of Medicine, New York, NY 10016, USA

[3]Department of Neuroscience & Physiology, New York University Grossman School of Medicine, New York, NY 10016, USA

[4]Lead contact

SUMMARY

Somatodendritic dopamine (DA) release from midbrain DA neurons activates D2 autoreceptors on these cells to regulate their activity. However, the source of autoregulatory DA remains controversial. Here, we test the hypothesis that D2 autoreceptors on a given DA neuron in the substantia nigra pars compacta (SNc) are activated primarily by DA released from that same cell, rather than from its neighbors. Voltage-clamp recording allows monitoring of evoked D2-receptor-mediated inhibitory currents (D2ICs) in SNc DA neurons as an index of DA release. Single-cell application of antibodies to Na^+ channels via the recording pipette decreases spontaneous activity of recorded neurons and attenuates evoked D2ICs; antibodies to SNAP-25, a soluble N-ethylmaleimide-sensitive factor attachment protein receptor (SNARE) protein, also decrease D2IC amplitude. Evoked D2ICs are nearly abolished by the light chain of botulinum neurotoxin A, which cleaves SNAP-25, whereas synaptically activated $GABA_B$-receptor-mediated currents are unaffected. Thus, somatodendritic DA release in the SNc autoinhibits the neuron that releases it.

In brief

Somatodendritic dopamine (DA) release inhibits DA neuron activity via D2 autoreceptors. A prevailing hypothesis is that this is mediated by synaptic release from neighboring DA neurons.

This is an open access article under the CC BY-NC-ND license (http://creativecommons.org/licenses/by-nc-nd/4.0/).

*Correspondence: margaret.rice@nyu.edu.

AUTHOR CONTRIBUTIONS

T.H. and M.E.R. designed experiments; T.H. and C.R.L. conducted whole-cell recording experiments; P.W. and J.C conducted immunocytochemical studies; K.I. created and provided BoNT/A light chain, BoNT/A holotoxin, and insight into sample preparation and design of BoNT/A controls; T.H., P.W., and M.E.R. wrote the manuscript with input from all other authors.

DECLARATION OF INTERESTS

K.I. is the founder of and has financial interests in CytoDel, Inc., a biopharmaceutical company with license to NYU patents that protect the work related to BoNT/A constructs used in this report.

SUPPLEMENTAL INFORMATION

Supplemental information can be found online at https://doi.org/10.1016/j.celrep.2021.108951.

Author Manuscript Author Manuscript Author Manuscript Author Manuscript

Hikima et al. show instead that a given SNc DA neuron is regulated by its own released DA, thus exhibiting true autoinhibition.

Graphical Abstract

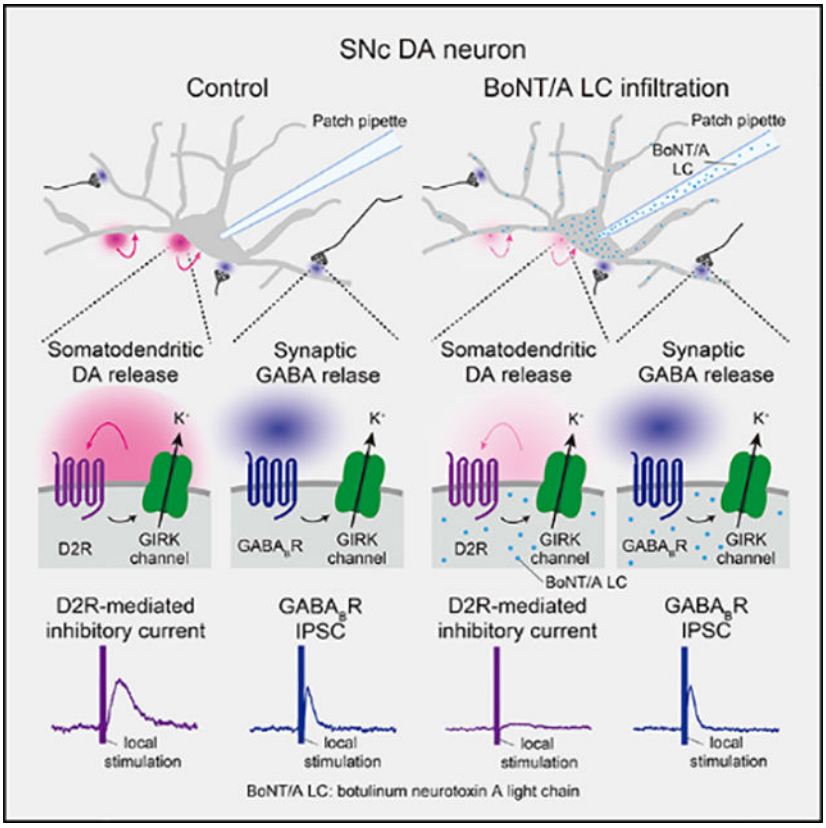

INTRODUCTION

Dopamine (DA) is involved in the regulation of movement and motivation (Mohebi et al., 2019; da Silva et al., 2018; Howe and Dombeck, 2016; Jin and Costa, 2010). Alteration in DA transmission is implicated in neuropsychiatric disorders like Parkinson's disease, in which loss of midbrain DA neurons in the substantia nigra pars compacta (SNc) leads to motor deficits, including decreased movement speed and amplitude (Albin et al., 1989; Carlsson, 2002).

In addition to axonal DA release in target regions, midbrain DA neurons release DA from their somata and dendrites in the SNc and in the adjacent ventral tegmental area (VTA) (Geffen et al., 1976; Rice and Patel, 2015; Gantz et al., 2018). Axonal DA released in the striatum acts at D2 autoreceptors to inhibit DA release (Sulzer et al., 2016). Similarly, somatodendritic DA activates D2 receptors on DA neurons, which inhibit spike firing via G-protein-coupled inwardly rectifying K^+ (GIRK) channels (Beckstead et al., 2004, 2007; Inanobe et al., 1999; Lacey et al., 1988; Pucak and Grace, 1994). This autoregulatory feedback pauses DA neuron firing and curtails axonal DA release (e.g., after a firing burst

Author Manuscript Author Manuscript Author Manuscript Author Manuscript

that accompanies initiation of a motor sequence or the receipt of an unexpected reward) (Fiorillo et al., 2003; Gerfen and Surmeier, 2011; Jin and Costa, 2010; Sulzer et al., 2016). Additionally, somatodendritically released DA acts at DA heteroreceptors in the substantia nigra pars reticulata (SNr), where it helps regulate motor output (Bergquist et al., 2003; Crocker, 1997; Zhou et al., 2009). Somatodendritic DA release is thus a pivotal intrinsic component of DA neuron function.

Somatodendritic DA release can be studied by stimulating DA neurons and monitoring the resulting D2-receptor-mediated inhibitory current (D2IC) from GIRK channel activation as a "biosensor" for DA release (Beckstead et al., 2004, 2007; Courtney et al., 2012; Ford et al., 2009, 2010; Gantz et al., 2013). The proposed source of DA for D2 receptor activation in both SNc and VTA is somatodendritic release at dendro-dendritic synapses between neighboring DA neurons (Beckstead et al., 2004; Courtney et al., 2012; Ford, 2014; Ford et al., 2010; Gantz et al., 2013, 2018). D2ICs are thus considered to be inhibitory postsynaptic currents (IPSCs). This interpretation, however, neglects important anatomical differences between DA neurons in the SNc and in the VTA. Dendro-dendritic synapses between DA neurons are rare in the SNc and are absent between neighboring DA dendrites in the SNr (Groves et al., 1975; Wassef et al., 1981). Moreover, immunohistochemical studies show clustered plasmalemmal DA transporter labeling near appositions between DA dendrites in the VTA but not in the SNc (Nirenberg et al., 1996b, 1997). In the VTA, DA release can also arise from axon collaterals (Bayer and Pickel, 1990; Deutch et al., 1988; Nirenberg et al., 1997), which adds a synapatic component to DA release in that region (Chen et al., 2011). By contrast, SNc DA neurons lack axon collaterals (Juraska et al., 1977; Nirenberg et al., 1996b; Wassef et al., 1981).

Here, we tested the hypothesis that a given SNc DA neuron is regulated primarily by its own DA release, rather than by synaptically released DA from neighboring neurons. We monitored D2ICs from voltage-clamped DA neurons in *ex vivo* midbrain slices and applied agents through the pipette that affected only the patch-clamped cell. Intracellular application of antibodies to Na^+ channels decreased the excitability of the recorded neuron and attenuated evoked D2ICs in that cell. Moreover, application of botulinum neurotoxin A (BoNT/A) light chain (LC/A), which cleaves SNAP-25, nearly abolished evoked D2ICs in recorded neurons but had no effect on synaptically activated $GABA_B$-receptor-mediated IPSCs. Our data thus indicate that somatodendritic DA release in SNc is a true *auto*regulatory signal.

RESULTS

Detection and function of somatodendritic DA release

D2ICs were evoked by local electrical stimulation (40 Hz, 5 pulses) at 4-min intervals in a cocktail of antagonists for $GABA_A$, $GABA_B$, N-methyl-D-aspartate (NMDA), and α-amino-3-hydroxy-5-methyl-4-isoxazolepropionic acid (AMPA) receptors (Beckstead et al., 2004). Peak D2IC amplitude was seen 0.2–0.5 s after the stimulus and returned to baseline within 2 s (Figure 1A). Evoked D2ICs were completely blocked by sulpiride (1 μM), a D2 receptor antagonist (Figure 1A), confirming pharmacological isolation of a DA-dependent current (Beckstead et al., 2004; Ford et al., 2009). We then examined the influence of locally

Author Manuscript Author Manuscript Author Manuscript Author Manuscript

evoked DA release on SNc neuron activity recorded in current-clamp mode. Spontaneous firing frequency of recorded SNc DA neurons was 1–5 Hz; the local stimulation protocol used to evoke D2ICs caused transient membrane hyperpolarization and a pause in spontaneous activity (Figure 1B), as reported previously (Beckstead et al., 2004, 2007; Courtney et al., 2012; Ford et al., 2010). The duration of the pause was coincident with that of D2ICs (Figure 1C) and was shortened by sulpiride (Figures 1B and 1D), confirming D2 receptor dependence. Thus, D2-autoreceptor feedback contributes to the temporal sculpting of DA neuron firing patterns in the SNc.

Single-cell inhibition of voltage-gated Na^+ channels decreases somatodendritic DA release in SNc

Somatodendritic DA release is activity dependent and tetrodotoxin sensitive (Chen et al., 2002; Robertson et al., 1991; Santiago et al., 1992). Here, we inhibited voltage-dependent Na^+ channel activity by intracellular application of antibodies against two Na^+ channel subtypes, $Na_v1.1$ and $Na_v1.2$, both of which are expressed by SNc DA neurons (Gong et al., 1999; González-Cabrera et al., 2017; see also Figure S1A). This single-cell approach allowed us to influence the spontaneous activity of the studied cell without affecting neighboring neurons. To confirm single-cell specificity of pipette application, we used immunohistochemical staining with a secondary antibody to localize Na_v Abs in tested cells after recording. These cells were filled with Neurobiotin 488 and identified as DA neurons by immunoreactivity (ir) for tyrosine hydroxylase (TH). Either $Na_v1.1$ Ab or $Na_v1.2$ Ab alone was tested in a given neuron ($Na_v1.1$ Ab, n = 5; $Na_v1.2$ Ab, n = 2); all seven recorded cells showed immunostaining for the tested antibody. The pattern of staining confirmed that Na_v Abs infiltrated the soma and proximal dendrites of DA neurons during the time of recording (20–25 min) and that the antibodies were confined to the recorded cell (Figures 2A and S1B).

We used current-clamp recording to compare effects on spontaneous activity in SNc DA neurons with single-cell application of Na_v Abs ($Na_v1.1$ Ab + $Na_v1.2$, 5 μg/mL each), vehicle only, or vehicle with control immunoglobulin G (IgG; 10 μg/mL). In contrast to the stability of firing rate in the two control groups (vehicle or IgG), the presence of Na_v Abs led to a progressive decrease in firing rate over a 25-min recording period, with a final frequency that was 14% ± 5% of initial (n = 7, $p < 0.01$ versus initial amplitude, paired t test) (Figures 2B and 2C). The range for initial frequency with Na_v Abs in the pipette was 1.2–3.4 Hz, which fell to 0–0.1 Hz (Figure 2D); there was no change in spontaneous frequency over the same period for vehicle or IgG controls (n = 5 per group) (Figure 2D). Spontaneous action potentials (APs) were completely lost in some cells (3/7) but persisted at a low frequency in others (4/7). Characteristics of persistent APs were largely indistinguishable from those recorded when the cell was first patched, except for a slight decrease in AP width at 50% peak amplitude (Figures S1C and S1D). The time to reach AP firing threshold from resting membrane voltage was also longer for these APs than those recorded immediately after patching (Figures 2E and 2F). We then examined neuronal excitability, indicated by AP number during depolarizing current injection. With Na_v Abs in the recording pipette, AP number fell within 10 min of patching, whereas AP number was stable in cells recorded with vehicle (Figures 2G–2I).

Author Manuscript Author Manuscript Author Manuscript Author Manuscript

We next assessed the influence of Na_v Abs on evoked somatodendritic DA release, indicated by a change in D2IC amplitude. We applied $Na_v1.1$ Ab or $Na_v1.2$ Ab individually (10 μg/mL) or together (5 μg/mL each). The decreases in D2IC amplitude seen at the time of maximal effect (28 min) did not differ significantly among individual or combined Na_v Abs application ($Na_v1.1$ Ab, 40% ± 11% decrease from initial, n = 3; $Na_v1.2$ Ab, 52% ± 3%, n = 3; $Na_v1.1$ + $Na_v1.2$ Abs, 57% ± 8%, n = 6; p = 0.5 one-way ANOVA). The data were therefore pooled, for an overall decrease in D2IC amplitude to 51% ± 5% of initial (n = 12, $p < 0.01$; paired t test) (Figures 3A–3C). In contrast, the final amplitude of evoked D2ICs with vehicle or IgG did not differ from initial amplitude (Figures 3A–3C). The time course of the decrease with Na_v Abs in the pipette was similar to that of the fall in SNc neuron excitability in current injection experiments (Figures 2H and 3A).

Given that GIRK2 channels underlie D2-receptor-mediated currents (Beckstead et al., 2004) and Na^+ entry regulates GIRK2 channel opening (Wang et al., 2016), we examined the influence of $Na_v1.1$ + $Na_v1.2$ Abs on D2IC kinetics, including time to peak, half width, and decay time (Figure S1E). None of these was altered, implying that the fall in D2IC amplitude reflected decreased DA release, rather than impaired GIRK channel regulation or function. As a further test, we evaluated the effect of each condition on D2 receptor currents elicited by a D2 receptor agonist, quinpirole. Superfusion of quinpirole (250 nM) for 15 s produced D2 currents of roughly the same amplitude as evoked D2ICs (Figure 3D). A second drug application at the end of the experiment revealed that quinpirole-induced currents were stable over the recording period with either vehicle or IgG (Figure 3E). These were also stable with Na_v Abs ($Na_v1.1$ Ab+ $Na_v1.2$ Ab, n = 4 or $Na_v1.1$ Ab only, n = 2; in the pipette [second quinpirole application 95% ± 8% of initial, n = 6, p = 0.7]; Figures 3D and 3E), whereas evoked D2IC amplitude in the same cells decreased to 57% ± 5% of initial (n = 6, $p < 0.01$).

Notably, this was not the case for an intracellular Na^+ channel blocker, QX-314 (Wilson and Kawaguchi, 1996), which has been reported to block GIRK channels at a high concentration (50 mM) (Andrade, 1991). We tested lower concentrations that might provide selective Na^+ channel blockade. Although QX-314 decreased evoked D2IC amplitude at concentrations as low as 5 mM (Figures S2A and S2C), quinpirole-induced currents were also decreased (Figures S2B and S2D). In contrast, the Na_v Abs had no effect on quinpirole-induced currents, allowing us to conclude that inhibition of Na^+ channel activity in a given SNc DA neuron decreases somatodendritic DA release from that cell.

Single-cell inhibition of SNAP-25 attenuates somatodendritic DA release

Although the mechanism of somatodendritic DA release is unresolved, the process appears to be exocytotic. Rat and guinea pig DA neurons express soluble N-ethylmaleimide-sensitive factor attachment protein receptor (SNARE) proteins, including membrane-associated SNAP-25, in the somatodendritic compartment (Fortin et al., 2006; Witkovsky et al., 2009). Moreover, exposure of DA neurons to BoNT/A, which cleaves SNAP-25, decreases somatodendritic DA release from DA neurons in culture and *in vivo* (Bergquist et al., 2003; Fortin et al., 2006). We identified SNAP-25 in mouse SNc DA neurons using immunohistochemistry, with detection of SNAP-25 ir in cell bodies and dendrites (sections

Author Manuscript Author Manuscript Author Manuscript Author Manuscript

from 18 mice) (Figure 4A) that was absent when the anti-SNAP-25 antibody (SNAP-25 Ab) was pre-incubated with its immunogenic peptide (IP) (Figure 4A), as reported previously for guinea pig SNc (Witkovsky et al., 2009). We next examined the effect of intracellular application of this SNAP-25 Ab on somatodendritic DA release. Evoked D2IC amplitude decreased significantly with SNAP-25 Ab (10 μg/mL) in the pipette (final D2IC amplitude 58% ± 4% of initial, n = 10, $p < 0.01$), whereas evoked D2ICs in time-matched control groups (vehicle or IgG) were stable (Figures 4B–4D).

We examined the influence of SNAP-25 Ab on D2IC kinetic properties, including time to peak, half width, and decay time (Figures 4E and S3). None of these properties was altered by intracellular vehicle or IgG (Figure S3). In contrast, the rise time (Figure S3) and time to peak (Figure 4E) of D2ICs were increased with SNAP-25 Ab (n = 8, time to peak, $p < 0.01$, rise time, $p < 0.05$; paired t test), without a change in half width or decay time (Figure S3). Quinpirole-induced currents were unaltered by SNAP-25 Ab in the pipette, indicating no effect on D2 receptors or GIRK channels (Figures 4F and 4G). Given the lack of change in the overall time course of D2ICs, which is governed primarily by D2-GIRK kinetics (Beckstead et al., 2007), the prolonged time to reach the peak presumably reflects the influence of SNAP-25 Ab on the release process.

This is not a consequence of lower DA release, as we found no correlation between peak amplitude and time to peak in D2ICs recorded under control conditions ($r = 0.1$; n = 37). The SNAP-25 Ab infiltrated the perikaryon and proximal dendrites of SNc DA neurons, indicated by immunohistochemistry using a secondary antibody to SNAP-25 Ab, with recorded cells identified by Neurobiotin 488 fluorescence and TH staining (Figure 4H). To test whether the effects of SNAP-25 Ab on D2IC amplitude might be influenced by leakage from the patch pipette to adjacent neurons, we positioned a patch pipette containing SNAP-25 Ab close to a presumed SNc DA neuron and maintained the usual holding current for 25 min before replacing the pipette with a recording pipette lacking SNAP-25 Ab to monitor evoked D2ICs from that cell (Figure S4A). In contrast to intracellular application of SNAP-25 Ab, prolonged extracellular SNAP-25 Ab ejection did not alter the amplitude of evoked D2ICs (Figures S4B–S4D) (final D2IC amplitude with extracellular SNAP-25 Ab: 102% ± 13% of initial, n = 6, $p = 0.6$; paired t test). The presence of SNAP-25 Ab adjacent to a recorded SNc DA neuron was confirmed using immunohistochemistry (Figure S4E). These data confirm single-cell effects of SNAP-25 Ab applied via the recording pipette and implicate SNAP-25 in somatodendritic DA release.

Single-cell application of LC/A prevents somatodendritic DA release

We utilized the bacterial protein BoNT/A from *Clostridium botulinum* (Montal, 2010) to test the role of SNAP-25 in somatodendritic DA release from the recorded cell further. Wild-type BoNT/A holotoxin consists of a disulfide-bonded heterodimer of light and heavy chains. The heavy chain binds to the cell surface, and BoNT/A holotoxin is endocytosed. After acidification in the early endosome, LC/A passes through the endosomal pore to neuronal cytoplasm, where it cleaves SNAP-25 (Montal, 2010). We bypassed the endocytotic step by direct, single-cell application of LC/A to SNc DA neurons. In contrast to the effect of $Na_v1.1$ Ab and $Na_v1.2$ Ab on DA neuron activity, intracellular LC/A (25 nM) did not alter

Author Manuscript Author Manuscript Author Manuscript Author Manuscript

spontaneous firing rate, even after 50 min of recording (Figures 5A and 5B). Initial frequency range was 1.7–3.4 Hz and was 1.1–5.9 Hz after 50 min of recording (n = 6, p = 0.9); LC/A had no effect on AP characteristics (Figure S5).

Nevertheless, intracellularly applied LC/A caused a marked decrease in D2IC amplitude (LC/A 34% ± 7%, n = 17, p < 0.001 versus initial amplitude) (Figures 5C–5E), demonstrating a key role for SNAP-25 in somatodendritic DA release. Time-matched control D2ICs recorded with either BoNT/A holotoxin or vehicle in the pipette remained stable over the recording period required for the maximal effect of LC/A (60 min) (final BoNT/A holotoxin: 90% ± 5% of initial, n = 10, p = 0.07; final vehicle: 98% ± 13% of initial, n = 12, p = 0.4) (Figures 5C–5E). Quinpirole-induced currents were unaltered by the intracellular LC/A (Figures 5F and 5G), as were those recorded with either BoNT/A holotoxin or vehicle (Figure 5G). In addition, LC/A decreased evoked D2ICs recorded in SNc DA neurons from females, as seen in males, confirming the generalizability of this result between sexes (Figure S6). Immunohistochemical identification of LC/A in recorded SNc DA neurons with an anti-LC/A antibody (Fan et al., 2015) showed LC/A ir throughout the cell bodies and, to a lesser extent, the dendrites of 4 of 5 neurons examined (Figure 5H). These data demonstrate that autoregulation in a given SNc DA neuron is mediated primarily by its own exocytotically released DA.

$GABA_B$ IPSCs are not affected by single-cell application of LC/A

The primary synaptic input to SNc DA neurons is GABAergic, which generates IPSCs mediated by $GABA_A$ and $GABA_B$ receptors (Lacey et al., 1988; Lobb et al., 2010). Synaptically evoked $GABA_B$-receptor-mediated currents are of particular relevance because, like D2ICs, they are mediated by GIRK channels (Beckstead et al., 2007; Davila et al., 2003; Lacey et al., 1988; Stuhrman and Roseberry, 2015). We compared the kinetics of pharmacologically isolated evoked D2ICs and $GABA_B$ IPSCs; D2IC isolation was described above, whereas $GABA_B$ IPSCs were isolated using antagonists for D2, $GABA_A$, NMDA, and AMPA receptors. Pharmacological isolation was confirmed by the loss of D2ICs with sulpiride (Figures 1A and 6A1) or loss of $GABA_B$ IPSCs with a $GABA_B$ receptor antagonist, CGP55845 (300 nM) (Figure 6A2). Stimulation intensities for evoked D2ICs and $GABA_B$ IPSCs did not differ (D2ICs, 48.5 ± 1.6 μA, n = 8; $GABA_B$ IPSCs, 45.0 ± 6.0 μA, n = 7; p = 0.6), nor did mean amplitudes of evoked D2ICs and $GABA_B$ IPSCs (D2ICs 28.3 ± 3.8 pA; $GABA_B$ IPSCs 22.3 ± 3.5 pA; p = 0.3; unpaired t test) (Figure 6B1). However, the time to peak for D2ICs was ~4-fold slower than for $GABA_B$ IPSCs (D2ICs, 283 ± 16 ms; $GABA_B$ IPSCs, 66 ± 7 ms; p < 0.001 unpaired t test) (Figure 6B2) and the decay time for D2ICs ~2.5-fold longer than for $GABA_B$ IPSCs (D2ICs, 436 ± 27 ms; $GABA_B$ IPSCs, 163 ± 9 ms; p < 0.001; unpaired t test) (Figure 6B3). The area under the curve (AUC) (pA*ms) for D2ICs was also greater than that for evoked $GABA_B$ IPSCs (D2IC, 15.4 ± 2.2 × 10^3; $GABA_B$ IPSCs, 3.9 ± 0.7 × 10^3; p < 0.001; unpaired t test) (Figure 6B4).

We examined the effect of single-cell application of LC/A on evoked $GABA_B$ IPSCs. If the effect of LC/A on evoked D2ICs reflected leakage to adjacent neurons, these IPSCs also should be impaired. However, in contrast to the decrease in evoked D2ICs (Figures 5C–5E), evoked $GABA_B$ IPSCs recorded with LC/A in the pipette did not change over 50 min of

Author Manuscript Author Manuscript Author Manuscript Author Manuscript

recording, with final $GABA_B$ IPSC amplitudes that were indistinguishable between vehicle and LC/A recording (vehicle, 88% ± 9%, n = 6, p = 0.12 versus initial; LC/A, 86% ± 16%, n = 7, p = 0.5 versus initial) (Figures 6C–6E).

Single-cell-evoked D2ICs

As a final test of our hypothesis that a given SNc DA neuron is regulated primarily its own DA release, we used a hybrid-clamp (HC) protocol to activate a given recorded SNc DA neuron (Oswald et al., 2009). The neuron is activated by current injection in current-clamp mode, then the amplifier is switched immediately to voltage clamp to detect D2ICs (Figure 7A). Using this approach, we obtained consistent D2-dependent currents that were inhibited by sulpiride (Figures 7A–7C). The peak time of D2ICs evoked in HC was comparable to that seen with local electrical stimulation (207 ± 14 ms, n = 5; Figure 7B), but the amplitude was lower (Figure 7C), possibly due to the absence of concurrently released transmitters acting at metabotropic receptors (Patel et al., 2009). We tested this using a metabotropic glutamate receptor (mGluR) antagonist, YM298198 (50 μM); mGluR antagonism caused a decrease in electrically evoked D2ICs compared to time-matched vehicle controls (vehicle, 115% ± 12% baseline, n = 5, p = 0.3; YM298198, 81% ± 5% baseline, n = 7, p < 0.05; paired t test) (Figure S7). These data indicate an amplification of DA release by endogenous glutamate with local stimulation that is absent with HC simulation of a single SNc DA neuron.

To assess whether a common DA source underlies D2ICs evoked by single-cell intracellular and local extracellular stimulation, we examined use-dependent depression of electrically evoked D2ICs after repetitive current stimulation in HC. We confirmed use-dependent depression of locally evoked D2ICs with repeated stimulation at 30-s intervals. In contrast to the stability of D2ICs evoked at 4-min intervals (Figures 3A, 4B, and 5C), D2IC amplitude decreased after only three stimulations (S1–S3) with 30-s intervals (n = 12, p < 0.01 S1 versus S3; p < 0.05 S2 versus S3; one-way ANOVA, Tukey post hoc test) (Figures 7D and 7E). We then examined the effect of three repetitions of HC stimulation at 30-s intervals on the amplitude of a subsequent D2IC evoked 30 s later; control recordings without HC stimulation were time-matched (Figure 7F). Consistent with a common cellular source of DA release, repetitive single-cell stimulation using HC also led to a use-dependent decrease in locally evoked D2IC amplitude, which recovered after a 4-min interval (post-HC stim D2IC, 72% ± 6% of pre-stim, n = 9, p < 0.05 and recovery 102% ± 11%, p = 0.9 versus pre-stim, one-way ANOVA, Tukey post hoc test; control, p = 0.9 at matched pre-stim time point and 0.4 for post-stim time point, n = 5; one-way ANOVA, Tukey post hoc test) (Figures 7F–7H). These data imply that DA is released from the same sites by either protocol, validating HC-evoked D2ICs.

DISCUSSION

Current thinking holds that somatodendritic DA release activates D2 autoreceptors at dendro-dendritic synapses in midbrain DA neurons, with DA-dependent currents reflecting postsynaptic D2 receptor activation (Beckstead et al., 2004, 2007; Courtney et al., 2012; Ford, 2014; Ford et al., 2010; Gantz et al., 2013, 2018). Here, using single-cell application

Author Manuscript Author Manuscript Author Manuscript Author Manuscript

of antibodies and other agents, we tested an alternative hypothesis: SNc DA neurons detect primarily their own DA release. We found that intracellular antibodies to Na^+ channels or SNAP-25 suppressed evoked somatodendritic DA release, reflected in decreased D2IC amplitude, without affecting currents induced by a D2 receptor agonist quinpirole. The most convincing evidence for DA autoregulation by the releasing cell was the loss of locally evoked D2ICs with single-cell application of LC/A, with no effect on quinpirole-induced currents. This interpretation is strengthened by the absence of effect of intracellular LC/A on synaptically evoked $GABA_B$ IPSCs in SNc DA neurons. The importance of D2 autoreceptor regulation of both somatodendritic and axonal DA release is reflected in consequences of selective D2 receptor deletion from DA neurons, including motor hyperactivity, increased motivation to work for food, and increased sensitivity to the psychostimulant effects of cocaine (Bello et al., 2011).

An intriguing aspect of somatodendritic DA release is that it differs in several ways from conventional synaptic transmission (Rice and Patel, 2015). For example, the Ca^{2+} dependence of DA release in the SNc differs markedly from axonal release, with persistence of release in low Ca^{2+} concentrations that do not support axonal release in striatum (Chen et al., 2011; Chen and Rice, 2001). We and others have also shown that SNc DA neurons express a different complement of SNARE proteins than that found at conventional fast synapses (Mendez et al., 2011; Witkovsky et al., 2009). The high sensitivity of somatodendritic DA release to Ca^{2+} provides an explanation for the persistence of somatodendritic DA release recorded with BAPTA (1,2-bis(o-aminophenoxy)ethane-N,N,N′,N′-tetraacetic acid) in the pipette, for example, as in the present studies.

AP dependence of somatodendritic DA release in SNc

It should be noted that SNc DA neurons have rapid, localized dendritic APs (Davie et al., 2006; Gentet and Williams, 2007) that are unclamped in our recording procedure, facilitating dendritic activation and DA release. The primary Na^+ channel subunits in SNc DA neurons are Na_v 1.1 and 1.2 (Ding et al., 2011; Gong et al., 1999; González-Cabrera et al., 2017). $Na_v1.2$ is widely expressed in SNc DA neurons, whereas $Na_v1.1$ detection is more variable (Ding et al., 2011; González-Cabrera et al., 2017). We found that $Na_v1.1$ and/or $Na_v1.2$ Abs in the pipette infiltrated the soma and proximal dendrites of SNc DA neurons and led to a significant suppression of spontaneous neuronal activity, neuronal excitability, and evoked D2IC amplitude. Our data are consistent with previous studies showing inhibition of somatodendritic DA release by tetrodotoxin (Beckstead et al., 2007; Chen and Rice, 2001; Santiago et al., 1992). Although the effect on D2IC amplitude and SNc neuron excitability was seen within 10 min of patching, a longer time was required for Na_v Abs to affect spontaneous AP generation. These data suggest that decreased excitability at the level of the cell body leads to decreased somatodendritic DA release. Biophysical features of SNc DA neurons provide a possible explanation for the longer time required for Na_v Abs to impair spontaneous APs. The axon of a SNc DA neuron arises from one of its dendrites (Blythe et al., 2009; Häusser et al., 1995), such that the Na^+-channel-dense initial segment (González-Cabrera et al., 2017) is distant from the source of Na_v Abs, increasing the time required to reach a concentration sufficient to impair AP generation.

Author Manuscript Author Manuscript Author Manuscript Author Manuscript

Given that somatodendritic DA release provides feedback inhibition that limits DA neuron activity and further DA release (Cragg and Greenfield, 1997; Gantz et al., 2013), the dependence of somatodendritic DA release on Na^+ channel activity makes mechanistic sense. This regulation is complemented by the Na^+ dependence of GIRK channel affinity for $G_{\beta\gamma}$ proteins (Petit-Jacques et al., 1999; Wang et al., 2016), which boosts autoinhibition by D2 receptors in a given SNc DA neuron under conditions of excess neuronal activity. Moreover, DA decreases the spontaneous activity of SNc DA neurons by inhibiting sodium leak channels in these cells (Philippart and Khaliq, 2018). In our studies, the lack of effect of Na_v Abs on quinpirole-induced currents indicates that they did not interfere with GIRK function. It is also unlikely that impaired Na^+ entry during stimulation contributed to the decrease in evoked D2IC amplitude, given that the Na^+ concentration in the pipette solution provides near-maximal $G_{\beta\gamma}$ protein affinity for GIRK channels (Wang et al., 2016). One final point is that several other Na^+ channels contribute to DA neuron excitability, including persistent Na^+ currents, which are sensitive to tetrodotoxin and contribute to the final phase of depolarization to the spike threshold (Ding et al., 2011; Khaliq and Bean, 2010; Puopolo et al., 2007). Although we cannot exclude an effect of Na_v Abs on persistent Na^+ currents, it would not alter our conclusion that SNc DA neuron excitability is a determining factor in somatodendritic DA release.

Compromising SNAP-25 in individual SNc neurons decreases somatodendritic DA release

Exocytotic transmitter release is a multistage process involving a network of synaptic proteins in vesicular and plasma membranes (Jahn and Fasshauer, 2012). SNAP-25 is associated with the plasma membrane and is a crucial component of the SNARE complex involved in conventional vesicle exocytosis (Fang et al., 2008; Jahn and Fasshauer, 2012; Takamori et al., 2006). We demonstrated a functional role for SNAP-25 using single-cell application of SNAP-25 Ab or LC/A, both of which target SNAP-25. Our data extend previous evidence for a role for SNAP-25 in somatodendritic DA release from DA neurons in culture and *in vivo* (Bergquist et al., 2003; Fortin et al., 2006). Although previous studies indicate that SNAP-25 can play a role in trafficking of receptors (e.g., AMPA receptors [Lledo et al., 1998; Lüscher et al., 1999] and GIRK channels [Koyrakh et al., 2005]), the lack of effect of SNAP-25 Ab or LC/A on quinpirole-induced D2 receptor currents implies a minimal role for SNAP-25 in D2 receptor or GIRK channel trafficking in SNc neurons.

Intracellular application of LC/A prevents somatodendritic D2ICs but not synaptic $GABA_B$ IPSCs

Both $GABA_B$ and D2 receptors activate GIRK channel-mediated K^+ currents (Lacey et al., 1988). However, the kinetics of the D2ICs and $GABA_B$ IPSCs differ (Figures 6A and 6B), consistent with different sites and regulation of transmitter release. Vesicular GABA is released from presynaptic terminals at conventional synapses with a GABA concentration decay time constant of ~500 μs (Overstreet et al., 2002). Synaptic concentrations of GABA, and, thus, the amplitude and duration of GABA IPSCs, are strongly regulated by GABA uptake into terminals and surrounding glial cells by GABA transporters that limit GABA spillover, with a time constant for synaptic GABA clearance of ~100 μs (Mozrzymas et al., 2003). Rapid GABA clearance helps ensure point-to-point transmission, with little crosstalk between neighboring synapses. In contrast, there is no evidence for clustering of vesicles or

Author Manuscript Author Manuscript Author Manuscript Author Manuscript

postsynaptic D2 receptors in SNc DA dendrites or somata (Nirenberg et al., 1996a; Robinson et al., 2017), implying a non-synaptic site of release. Additionally, DA uptake occurs only at sites on DA somata and dendrites, indicating a prominent role for regulation of post-release concentration by diffusion parameters specific to the SNc and SNr (Cragg et al., 2001; Rice and Cragg, 2008). Overall, these differences are consistent with a synaptic source of GABA for $GABA_B$ IPSCs and a non-synaptic source for D2ICs. We took advantage of these distinct transmitter sources by examining the effect of intracellular LC/A application on evoked DA and GABA currents. Near elimination of D2ICs, but no effect on synaptic $GABA_B$ IPSCs, is consistent with inhibition of DA release from the recorded cell and rules out the possibility that LC/A leaked from the pipette to inhibit synaptic release onto DA neurons.

Single-cell-evoked DA release in HC

Our evidence for a non-synaptic, activity-dependent DA source was bolstered by the detection of single-cell-evoked D2ICs using HC. Although the D2ICs evoked by HC were smaller than those evoked by local electrical stimulation, a common release mechanism and source of DA for the two methods was indicated by the ability of prior HC stimulation to depress subsequent D2ICs evoked by local stimulation (Figures 7F–7H). A likely contributing factor to smaller currents in HC is the absence of concurrently evoked transmitters that activate metabotropic receptors, promote Ca^{2+} release from intracellular stores, and boost somatodendritic DA release (Patel et al., 2009). In addition to mGluRs (Figure S7), activation of nicotinic, muscarinic, and α1 noradrenergic receptors on SNc DA neurons (Estakhr et al., 2017; Foster et al., 2014; Grenhoff et al., 1995) might boost DA release. Lower D2IC amplitude might also reflect limited dendritic activation in HC. Local electrical stimulation depolarizes dendrites as well as somata, which is an advantage for studying the release process, as dendrites are key sites of DA release (Cheramy et al., 1981). Dendrites also receive abundant synaptic input for modulation of DA release; mGluRs, for example, are more highly expressed on SNc DA dendrites than somata (Hubert et al., 2001). Additionally, the efficacy of AP backpropagation into non-axon-bearing SNc DA dendrites with somatic depolarization is variable. Some studies find that APs and Ca^{2+} signals from SNc cell bodies propagate to dendrites (Hage and Khaliq, 2015; Häusser et al., 1995), whereas others find variable fidelity and even propagation failure (Gentet and Williams, 2007), particularly at higher frequencies (Hage and Khaliq, 2015). Nevertheless, the present results show that stimulation of a single DA neuron is sufficient to induce DA release that activates inhibitory D2 receptors on the recorded cell.

Conclusions

We report that a SNc DA neuron is regulated primarily by its own DA release, rather than by synaptic DA release from its neighbors. Our conclusion is supported by the marked impairment of evoked D2ICs with intracellular active LC/A, but a lack of effect on synaptic $GABA_B$ IPSCs, and the detection of D2R-dependent currents evoked with single-cell stimulation using HC. Our results do not exclude additional contributions from synaptically released DA, especially in the VTA, where axonal as well as dendro-dendritic DA synapses can release DA (Chen et al., 2011), or DA diffusion from nearby cells (Rice and Cragg, 2008). Although molecular diversity of SNc DA neurons is increasingly recognized (Lerner

Author Manuscript Author Manuscript Author Manuscript Author Manuscript

et al., 2015; Poulin et al., 2014), the detection of D2ICs in all recorded SNc DA neurons and sex-independent suppression of DA release by the various agents tested here implies that autoregulation by self-released DA is a general process in SNc DA neurons.

STAR★METHODS

RESOURCE AVAILABILITY

Lead contact—Further information and requests for reagents may be directed to the Lead Contact, Margaret E. Rice (margaret.rice@nyu.edu).

Materials availability—These studies did not generate unique reagents.

Data and code availability—No new datasets/code were generated.

EXPERIMENTAL MODEL AND SUBJECT DETAILS

Animals—All animal procedures conform to guidelines of the Institutional Animal Care and Use Committee at the New York University Grossman School of Medicine. In most experiments, male C57B6 wild-type mice (Jackson Laboratory, Stock no. 000664) aged 4 to 6 weeks postnatal were used; female mice of the same age were used to test the hypothesis that the basic effect of LC/A was sex independent. All mice were group housed with controlled temperature and humidity, and maintained on a 12:12 h light cycle (lights on at 06:30) with food and water *ad libitum* in an AAALAC-accredited facility.

Slice preparation—Mice were administered Euthasol (120 mg/kg pentobarbital, intraperitoneal, i.p.), then perfused transcardially with ice-cold cutting solution containing (in mM); 200 sucrose; 2.5 KCl; 26 $NaHCO_3$; 1.25 NaH_2PO_4; 0.5 $CaCl_2$; 7 $MgSO_4$; 1 ascorbic acid; 3 sodium pyruvate; 7 glucose; the solution was equilibrated with 95% O_2/5% CO_2 (Lee et al., 2013). Brains were removed and placed in ice-cold cutting solution. Horizontal midbrain slices (250 μm thick) were cut on a Leica VT1200S vibrating microtome (Leica Microsystems, Buffalo Grove, IL, USA), transferred to a holding chamber for 40 min at 35°C, then maintained at least 30 min at room temperature in artificial CSF (aCSF) containing (in mM): 125 NaCl; 2.5 KCl; 25 $NaHCO_3$; 1.25 NaH_2PO_4; 2 $CaCl_2$; 1 $MgSO_4$; 1 sodium ascorbate; 3 sodium pyruvate; 25 glucose; 0.4 myo-inositol (Lee et al., 2013). Experimental slices were transferred to the recording chamber and superfused at 1.2 mL/min with 32°C bicarbonate-buffered aCSF, containing (in mM): 124 NaCl; 3.7 KCl; 26 $NaHCO_3$; 2.4 $CaCl_2$; 1.3 $MgSO_4$; 1.3 KH_2PO_4 and 10 glucose equilibrated with 95% O_2/5% CO_2.

METHOD DETAILS

Electrophysiology—A Multiclamp 700B or Axopatch 200B with a Digidata 1550B converter and Clampex10.7 software (Molecular Devices, San Jose, CA, USA) was used for whole-cell recording. The landmark to identify SNc in midbrain slices was the medial terminal nucleus of the accessory optic tract. Using an Olympus BX50WI microscope (Olympus America, Center Valley, PA, USA) with IR-DIC optics, SNc DA neurons were recognized by their large spindle-shaped cell bodies, then physiologically identified by a low

Author Manuscript Author Manuscript Author Manuscript Author Manuscript

spontaneous spike rate (1–5Hz), action potential width of > 1.2 ms recorded in voltage-clamp, and the presence of an *h*-current (> 200 pA) elicited in response to a shift in membrane voltage from −60 mV to −110 mV (Ford et al., 2006).

For voltage-clamp recording of D2ICs or $GABA_B$ IPSCs, neurons were held at −60 mV; currents were filtered at 2 kHz and digitized at 10 kHz; pipette resistance was 2.0–3.5 MΩ. The pipette solution contained (in mM): 115 K-methylsulfate; 20 NaCl; 1.5 $MgCl_2$; 5 HEPES; 10 BAPTA or 10 EGTA; 3 Na_2-ATP; 0.3 Na_3-GTP, pH 7.3 with KOH, 291–300 mOsm (Ford et al., 2010). BAPTA-based internal solutions for voltage clamp were used to minimize D2 receptor desensitization (Robinson et al., 2017). For current-clamp recording, the pipette solution contained (in mM): 120 K-gluconate; 20 KCl; 2 $MgCl_2$; 10 HEPES; 10 EGTA; 3 Na_2-ATP; 0.2 Na_3-GTP, pH 7.3 with KOH, 300 mOsm. For pharmacological isolation of D2ICs, picrotoxin (100 μM), CGP55845 (0.3 μM), 6,7-dinitroquinoxaline-2,3-dione (DNQX; 10 μM) and D-2-amino-phosphonopentanoic acid (D-AP5; 50 μM) were included in the recording aCSF; isolation of $GABA_B$ IPSCs, the same antagonists were included, except that the $GABA_B$R antagonist CGP55845 was omitted and sulpiride (1 μM) included. A bipolar stimulating electrode (FHC, Bowdoin, ME, USA) was placed on the slice surface, 50–100 μm lateral to the neuron; D2ICs or $GABA_B$ IPSCs were evoked by a 5-pulse train at 40 Hz at 4 min intervals; stimulus intensity was 16–90 μA for D2ICs and 15–80 μA for $GABA_B$ IPSCs. Voltage-clamp recording of quinpirole-induced currents was used to assess D2 receptor-GIRK function; given that quinpirole can desensitize D2Rs (Robinson et al., 2017), we optimized quinpirole concentration (250 nM) and application time (15 s) to achieve a reproducible current that did not affect subsequent evoked D2ICs. Series resistances were not compensated; recordings were discarded if the series resistance exceeded 15 MΩ. Electrodes were prepared from glass capillaries (Sutter Instruments Company, Novato, CA, USA) with a horizontal micropipette puller (P-97, Sutter Instruments).

In some experiments, Neurobiotin 488 (0.006%–0.02%) plus either Na_v 1.1 Ab and/or Na_v 1.2 Ab (5 μg/mL each when applied together, or 10 μg/mL when tested separately), rabbit IgG (10 μg/mL), SNAP-25 Ab (10 μg/mL), or LC/A or BoNT/A holotoxin (25 nM each) were included in pipette solutions. The LC/A protein (1–427 amino acids) was expressed in *Escherichia coli* and purified by Dr. Ichtchenko using methods described previously (Baldwin et al., 2004). Vehicle for Na_v Abs, IgG and SNAP-25 Ab was phosphate buffered saline (PBS) containing 1% BSA; 0.05% NaN_3, pH 7.4. Vehicle for BoNT/A contained zinc acetate (25 nM). To assess effects of these intracellularly applied agents, initial records were taken within 5 min of patching with continual monitoring until a stable maximal effect was seen (28–60 min). Control measurements (e.g., vehicle or IgG) were time-matched to the duration required for an active agent. All epitopes targeted by the antibodies used were intracellular. The Na_v1.1 antibody (Alomone Labs, #ASC-001) was raised against the peptide (C)TASEHSREPSAAGRLSD, corresponding to amino acid residues 465–481 of Na_v1.1 intracellular loop between domains I and II. Specificity was shown by the absence of immunostaining in brain tissue from Na_v1.1 knockout mice (Kalume et al., 2015), and supported by the absence of staining after preadsorption with its immunogenic peptide (Figure S1A). The Na_v1.2 antibody (Alomone Labs, #ASC-002) was raised against the peptide (C)ASAESRDFSGAGGIGVFSE, corresponding to amino acid residues 467–485 of

Author Manuscript Author Manuscript Author Manuscript Author Manuscript

Na_v 1.2 intracellular loop between domains I and II. Specificity was shown by the absence of western blot staining from $Na_v1.2$ knockout mice (Planells-Cases et al., 2000). The SNAP-25 Ab (Synaptic Systems, #111–002) was raised against the peptide (C)IDEANQRATKMLGSG, corresponding to amino acid resides 192 −206 of SNAP-25 intracellular position. This antibody recognizes SNAP-25a and b isoforms, with SNAP-25b being the predominant isoform in brain; specificity was shown by the absence of staining in western blots from SNAP-25b knockout mice (Irfan et al., 2019). To test whether leakage from a recording pipette containing SNAP-25 Ab (10 μg/mL) might contribute to decreases in D2IC amplitude seen with SNAP-25 Ab applied intracellularly, a pipette containing SNAP-25 was positioned near a presumed SNc DA neuron and positive pressure (~3 mbar, monitored by manometer) applied for 25 min. This pipette was then replaced with a recording electrode containing Neurobiotin 488 (0.006%) but not SNAP-25, the DA neuron patched and identified, and D2ICs evoked as usual.

For hybrid-clamp recording, the pipette solution contained (in mM): 120 K-gluconate; 20 KCl; 2 $MgCl_2$; 10 HEPES; 10 BAPTA; 3 Na_2-ATP; 0.2 Na_3-GTP, pH 7.3 with KOH, 300 mOsm. When hybrid-clamp was used to evoke D2ICs, current-clamp pulses (5 pulses, 40 Hz; 400 pA, 8 ms duration) were applied, then recording switched to voltage-clamp (holding voltage, −50 mV) was triggered 20 ms after the stimulus pulses.

Immunohistochemistry—Immunohistochemical staining was used to confirm the presence of Na_v channels and SNAP-25 in mouse SNc DA neurons, and to determine the extent of infiltration of antibodies to these proteins or of LC/A during whole-cell recording in *ex vivo* midbrain slices. For cellular identification, mice were injected with Euthasol (120 mg/kg, i.p.) and perfused transcardially with PBS followed by freshly prepared 4% paraformaldehyde (PFA) in 0.1 M phosphate buffer, pH 7.2. Brains were removed, post-fixed in phosphate buffered PFA overnight, and cryoprotected in 20% sucrose, then 30% sucrose. Frozen coronal sections (50 μm thick) were cut in a Cryocut 1800 cryostat (Belair Instrument Company, Springfield, NJ, USA) and processed for immunohistochemistry.

Brain sections were washed 3 × 15 min in PBS + 0.1% Triton X-100, then 1 h in 5% donkey serum in PBS + 0.3% Triton X-100 followed by incubation in the primary antibodies for 18–24 h at room temperature on a rotating platform. Sections were washed 3 × 15 min in PBS/0.3% Triton X-100, then incubated in secondary antibodies diluted 1:200 for 2 h. After final washes in PBS alone, sections were mounted on slides, air-dried, dehydrated in graded alcohols, treated with Citrisolv and coverslipped in Krystalon (EMD Chemicals Inc, Gibbstown, NJ, USA). In experiments in which Neurobiotin488 was included in the pipette test slices were transferred immediately after recording to a chilled solution of 4% paraformaldehyde in PBS and stored overnight at 4°C. Similar procedures were used for PFA-fixed experimental brain slices, except that whole slices were mounted with Vectashield (Vector Laboratories Inc) without dehydration and exposure to Citrisolv. In addition to the Nav1.1 and 1.2 and SNAP-25 Abs described above, specificity of the monoclonal Ab against LC/A has been shown in extensive characterization studies (Fan et al., 2015), and the polyclonal TH Ab has been used extensively, and selectively immunostains DA neurons indicated by colocalization with other biogenic amine neurons markers like the vesicular

Author Manuscript Author Manuscript Author Manuscript Author Manuscript

monoamine transporter (VMAT2) (Witkovsky et al., 2009). Primary and secondary antibodies are listed in the Key Resources Table.

Images of immunostained tissue were obtained with a Nikon Eclipse C1 confocal microscope and processed with Photoshop (Adobe Systems Incorporated, San Jose, CA, USA) or ImageJ (NIH). Any changes in brightness and/or contrast were made on the entire image. Comparisons of immunostained control and preabsorbed tissue were on adjacent sections from the same brain, using identical confocal photomultiplier settings. Each primary antibody was tested on tissue from least two mice.

Chemicals and drugs—BAPTA, EGTA and picrotoxin were purchased from Sigma-Aldrich (Saint Louis, MO, USA); D-AP5, DNQX, CGP55845, sulpiride and quinpirole were from Tocris (Minneapolis, MN, USA); BoNT/A holotoxin was from Metabiologics (Madison, WI, USA).

QUANTIFICATION AND STATISTICAL ANALYSIS

Electrophysiological data were obtained and quantified using pClamp10 (Molecular Devices), then analyzed and graphed with Clampfit (Molecular Device) and Graphpad Prism (GraphPad Software Inc, San Diego, CA, USA). Data are reported as means ± SEM; n = number of cells. Kinetic parameters for D2IC and $GABA_B$ IPSCs were determined from an average of at least three measurements per cell. AUC was determined from the start of the current rise to the end, and expressed as pA*ms. Decay time was estimated from an exponential function. Rise time was the time required for the rising phase to increase from 20% to 80% of peak amplitude. Duration of the pause in spontaneous frequency after stimulation was measured from the end of last stimulation pulse to time of the peak of the initial spontaneous spike after the stimulus. Resting membrane potential was estimated as the inflection in the membrane potential between the offset of the afterhyperpolarization and the initiation of the next slow depolarization (Grace and Onn, 1989). Differences for within-group comparisons was assessed by paired two-tailed t tests, and between two groups by unpaired two-tailed t tests for all analysis. Differences among three experimental groups was determined by one-way ANOVA followed by Tukey post hoc test. Statistical significance was considered $p < 0.05$.

Supplementary Material

Refer to Web version on PubMed Central for supplementary material.

ACKNOWLEDGMENTS

Funding was provided by the Marlene and Paolo Fresco institute for Parkinson's Disease and Movement Disorders and by NIH R01 DA038616 (M.E.R.) and R01 AI093504 (K.I.). We are grateful to Drs. John N.J. Reynolds and Manfred J. Oswald for insightful discussions about hybrid-clamp recording. The author list of this paper includes contributors from the location where the research was conducted who participated in the data collection, design, analysis, and/or interpretation of the work.

Author Manuscript Author Manuscript Author Manuscript Author Manuscript

REFERENCES

Albin RL, Young AB, and Penney JB (1989). The functional anatomy of basal ganglia disorders. Trends Neurosci. 12, 366–375. [PubMed: 2479133]

Andrade R (1991). Blockade of neurotransmitter-activated K^+ conductance by QX-314 in the rat hippocampus. Eur. J. Pharmacol 199, 259–262. [PubMed: 1659537]

Baldwin MR, Bradshaw M, Johnson EA, and Barbieri JT (2004). The C-terminus of botulinum neurotoxin type A light chain contributes to solubility, catalysis, and stability. Protein Expr. Purif 37, 187–195. [PubMed: 15294297]

Bayer VE, and Pickel VM (1990). Ultrastructural localization of tyrosine hydroxylase in the rat ventral tegmental area: relationship between immunolabeling density and neuronal associations. J. Neurosci 10, 2996–3013. [PubMed: 1975839]

Beckstead MJ, Grandy DK, Wickman K, and Williams JT (2004). Vesicular dopamine release elicits an inhibitory postsynaptic current in midbrain dopamine neurons. Neuron 42, 939–946. [PubMed: 15207238]

Beckstead MJ, Ford CP, Phillips PEM, and Williams JT (2007). Presynaptic regulation of dendrodendritic dopamine transmission. Eur. J. Neurosci 26, 1479–1488. [PubMed: 17822435]

Bello EP, Mateo Y, Gelman DM, Noaín D, Shin JH, Low MJ, Alvarez VA, Lovinger DM, and Rubinstein M (2011). Cocaine supersensitivity and enhanced motivation for reward in mice lacking dopamine D2 autoreceptors. Nat. Neurosci 14, 1033–1038. [PubMed: 21743470]

Bergquist F, Shahabi HN, and Nissbrandt H (2003). Somatodendritic dopamine release in rat substantia nigra influences motor performance on the accelerating rod. Brain Res. 973, 81–91. [PubMed: 12729956]

Blythe SN, Wokosin D, Atherton JF, and Bevan MD (2009). Cellular mechanisms underlying burst firing in substantia nigra dopamine neurons. J. Neurosci 29, 15531–15541. [PubMed: 20007477]

Carlsson A (2002). Treatment of Parkinson's with L-DOPA. The early discovery phase, and a comment on current problems. J. Neural Transm. (Vienna) 109, 777–787. [PubMed: 12111467]

Chen BT, and Rice ME (2001). Novel Ca^{2+} dependence and time course of somatodendritic dopamine release: substantia nigra versus striatum. J. Neurosci 21, 7841–7847. [PubMed: 11567075]

Chen BT, Avshalumov MV, and Rice ME (2002). Modulation of somatodendritic dopamine release by endogenous H(2)O(2): susceptibility in substantia nigra but resistance in VTA. J. Neurophysiol 87, 1155–1158. [PubMed: 11826083]

Chen BT, Patel JC, Moran KA, and Rice ME (2011). Differential calcium dependence of axonal versus somatodendritic dopamine release, with characteristics of both in the ventral tegmental area. Front. Syst. Neurosci 5, 39. [PubMed: 21716634]

Cheramy A, Leviel V, and Glowinski J (1981). Dendritic release of dopamine in the substantia nigra. Nature 289, 537–542. [PubMed: 6258083]

Courtney NA, Mamaligas AA, and Ford CP (2012). Species differences in somatodendritic dopamine transmission determine D2-autoreceptor-mediated inhibition of ventral tegmental area neuron firing. J. Neurosci 32, 13520–13528. [PubMed: 23015441]

Cragg SJ, and Greenfield SA (1997). Differential autoreceptor control of somatodendritic and axon terminal dopamine release in substantia nigra, ventral tegmental area, and striatum. J. Neurosci 17, 5738–5746. [PubMed: 9221772]

Cragg SJ, Nicholson C, Kume-Kick J, Tao L, and Rice ME (2001). Dopamine-mediated volume transmission in midbrain is regulated by distinct extracellular geometry and uptake. J. Neurophysiol 85, 1761–1771. [PubMed: 11287497]

Crocker AD (1997). The regulation of motor control: an evaluation of the role of dopamine receptors in the substantia nigra. Rev. Neurosci 8, 55–76. [PubMed: 9402645]

da Silva JA, Tecuapetla F, Paixão V, and Costa RM (2018). Dopamine neuron activity before action initiation gates and invigorates future movements. Nature 554, 244–248. [PubMed: 29420469]

Davie JT, Kole MHP, Letzkus JJ, Rancz EA, Spruston N, Stuart GJ, and Häusser M (2006). Dendritic patch-clamp recording. Nat. Protoc 1, 1235–1247. [PubMed: 17406407]

Author Manuscript Author Manuscript Author Manuscript Author Manuscript

Davila V, Yan Z, Craciun LC, Logothetis D, and Sulzer D (2003). D_3 dopamine autoreceptors do not activate G-protein-gated inwardly rectifying potassium channel currents in substantia nigra dopamine neurons. J. Neurosci 23, 5693–5697. [PubMed: 12843272]

Deutch AY, Goldstein M, Baldino F Jr., and Roth RH (1988). Telencephalic projections of the A8 dopamine cell group. Ann. N Y Acad. Sci 537, 27–50. [PubMed: 2462395]

Ding S, Wei W, and Zhou F-M (2011). Molecular and functional differences in voltage-activated sodium currents between GABA projection neurons and dopamine neurons in the substantia nigra. J. Neurophysiol 106, 3019–3034. [PubMed: 21880943]

Estakhr J, Abazari D, Frisby K, McIntosh JM, and Nashmi R (2017). Differential control of dopaminergic excitability and locomotion by cholinergic inputs in mouse substantia nigra. Curr. Biol 27, 1900–1914.e4. [PubMed: 28648825]

Fan Y, Geren IN, Dong J, Lou J, Wen W, Conrad F, Smith TJ, Smith LA, Ho M, Pires-Alves M, et al. (2015). Monoclonal antibodies targeting the alpha-exosite of botulinum neurotoxin serotype/A inhibit catalytic activity. PLoS ONE 10, e0135306. [PubMed: 26275214]

Fang Q, Berberian K, Gong L-W, Hafez I, Sørensen JB, and Lindau M (2008). The role of the C terminus of the SNARE protein SNAP-25 in fusion pore opening and a model for fusion pore mechanics. Proc. Natl. Acad. Sci. USA 105, 15388–15392. [PubMed: 18829435]

Fiorillo CD, Tobler PN, and Schultz W (2003). Discrete coding of reward probability and uncertainty by dopamine neurons. Science 299, 1898–1902. [PubMed: 12649484]

Ford CP (2014). The role of D2-autoreceptors in regulating dopamine neuron activity and transmission. Neuroscience 282, 13–22. [PubMed: 24463000]

Ford CP, Mark GP, and Williams JT (2006). Properties and opioid inhibition of mesolimbic dopamine neurons vary according to target location. J. Neurosci 26, 2788–2797. [PubMed: 16525058]

Ford CP, Phillips PEM, and Williams JT (2009). The time course of dopamine transmission in the ventral tegmental area. J. Neurosci 29, 13344–13352. [PubMed: 19846722]

Ford CP, Gantz SC, Phillips PEM, and Williams JT (2010). Control of extracellular dopamine at dendrite and axon terminals. J. Neurosci 30, 6975–6983. [PubMed: 20484639]

Fortin GD, Desrosiers CC, Yamaguchi N, and Trudeau L-É (2006). Basal somatodendritic dopamine release requires snare proteins. J. Neurochem 96, 1740–1749. [PubMed: 16539689]

Foster DJ, Gentry PR, Lizardi-Ortiz JE, Bridges TM, Wood MR, Niswender CM, Sulzer D, Lindsley CW, Xiang Z, and Conn PJ (2014). M_5 receptor activation produces opposing physiological outcomes in dopamine neurons depending on the receptor's location. J. Neurosci 34, 3253–3262. [PubMed: 24573284]

Gantz SC, Bunzow JR, and Williams JT (2013). Spontaneous inhibitory synaptic currents mediated by a G protein-coupled receptor. Neuron 78, 807–812. [PubMed: 23764286]

Gantz SC, Ford CP, Morikawa H, and Williams JT (2018). The evolving understanding of dopamine neurons in the substantia nigra and ventral tegmental area. Annu. Rev. Physiol 80, 219–241. [PubMed: 28938084]

Geffen LB, Jessell TM, Cuello AC, and Iversen LL (1976). Release of dopamine from dendrites in rat substantia nigra. Nature 260, 258–260. [PubMed: 1256567]

Gentet LJ, and Williams SR (2007). Dopamine gates action potential backpropagation in midbrain dopaminergic neurons. J. Neurosci 27, 1892–1901. [PubMed: 17314285]

Gerfen CR, and Surmeier DJ (2011). Modulation of striatal projection systems by dopamine. Annu. Rev. Neurosci 34, 441–466. [PubMed: 21469956]

Gong B, Rhodes KJ, Bekele-Arcuri Z, and Trimmer JS (1999). Type I and type II Na^+ channel α-subunit polypeptides exhibit distinct spatial and temporal patterning, and association with auxiliary subunits in rat brain. J. Comp. Neurol 412, 342–352. [PubMed: 10441760]

González-Cabrera C, Meza R, Ulloa L, Merino-Sepúlveda P, Luco V, Sanhueza A, Oñate-Ponce A, Bolam JP, and Henny P (2017). Characterization of the axon initial segment of mice substantia nigra dopaminergic neurons. J. Comp. Neurol 525, 3529–3542. [PubMed: 28734032]

Grace AA, and Onn S-P (1989). Morphology and electrophysiological properties of immunocytochemically identified rat dopamine neurons recorded in vitro. J. Neurosci 9, 3463–3481. [PubMed: 2795134]

Author Manuscript Author Manuscript Author Manuscript Author Manuscript

Grenhoff J, North RA, and Johnson SW (1995). Alpha 1-adrenergic effects on dopamine neurons recorded intracellularly in the rat midbrain slice. Eur. J. Neurosci 7, 1707–1713. [PubMed: 7582125]

Groves PM, Wilson CJ, Young SJ, and Rebec GV (1975). Self-inhibition by dopaminergic neurons. Science 190, 522–528. [PubMed: 242074]

Hage TA, and Khaliq ZM (2015). Tonic firing rate controls dendritic Ca^{2+} signaling and synaptic gain in substantia nigra dopamine neurons. J. Neurosci 35, 5823–5836. [PubMed: 25855191]

Häusser M, Stuart G, Racca C, and Sakmann B (1995). Axonal initiation and active dendritic propagation of action potentials in substantia nigra neurons. Neuron 15, 637–647. [PubMed: 7546743]

Howe MW, and Dombeck DA (2016). Rapid signalling in distinct dopaminergic axons during locomotion and reward. Nature 535, 505–510. [PubMed: 27398617]

Hubert GW, Paquet M, and Smith Y (2001). Differential subcellular localization of mGluR1a and mGluR5 in the rat and monkey Substantia nigra. J. Neurosci 21, 1838–1847. [PubMed: 11245668]

Inanobe A, Yoshimoto Y, Horio Y, Morishige K-I, Hibino H, Matsumoto S, Tokunaga Y, Maeda T, Hata Y, Takai Y, and Kurachi Y (1999). Characterization of G-protein-gated K^+ channels composed of Kir3.2 subunits in dopaminergic neurons of the substantia nigra. J. Neurosci 19, 1006–1017. [PubMed: 9920664]

Irfan M, Gopaul KR, Miry O, Hökfelt T, Stanton PK, and Bark C (2019). SNAP-25 isoforms differentially regulate synaptic transmission and long-term synaptic plasticity at central synapses. Sci. Rep 9, 6403. [PubMed: 31024034]

Jahn R, and Fasshauer D (2012). Molecular machines governing exocytosis of synaptic vesicles. Nature 490, 201–207. [PubMed: 23060190]

Jin X, and Costa RM (2010). Start/stop signals emerge in nigrostriatal circuits during sequence learning. Nature 466, 457–462. [PubMed: 20651684]

Juraska JM, Wilson CJ, and Groves PM (1977). The substantia nigra of the rat: a Golgi study. J. Comp. Neurol 172, 585–600. [PubMed: 65369]

Kalume F, Oakley JC, Westenbroek RE, Gile J, de la Iglesia HO, Scheuer T, and Catterall WA (2015). Sleep impairment and reduced interneuron excitability in a mouse model of Dravet Syndrome. Neurobiol. Dis 77, 141–154. [PubMed: 25766678]

Khaliq ZM, and Bean BP (2010). Pacemaking in dopaminergic ventral tegmental area neurons: depolarizing drive from background and voltage-dependent sodium conductances. J. Neurosci 30, 7401–7413. [PubMed: 20505107]

Koyrakh L, Luján R, Colón J, Karschin C, Kurachi Y, Karschin A, and Wickman K (2005). Molecular and cellular diversity of neuronal G-protein-gated potassium channels. J. Neurosci 25, 11468–11478. [PubMed: 16339040]

Lacey MG, Mercuri NB, and North RA (1988). On the potassium conductance increase activated by $GABA_B$ and dopamine D_2 receptors in rat substantia nigra neurones. J. Physiol 401, 437–453. [PubMed: 2459376]

Lee CR, Machold RP, Witkovsky P, and Rice ME (2013). TRPM2 channels are required for NMDA-induced burst firing and contribute to H(2)O(2)-dependent modulation in substantia nigra pars reticulata GABAergic neurons. J. Neurosci 33, 1157–1168. [PubMed: 23325252]

Lerner TN, Shilyansky C, Davidson TJ, Evans KE, Beier KT, Zalocusky KA, Crow AK, Malenka RC, Luo L, Tomer R, and Deisseroth K (2015). Intact-brain analyses reveal distinct information carried by SNc dopamine subcircuits. Cell 162, 635–647. [PubMed: 26232229]

Lledo P-M, Zhang X, Südhof TC, Malenka RC, and Nicoll RA (1998). Postsynaptic membrane fusion and long-term potentiation. Science 279, 399–403. [PubMed: 9430593]

Lobb CJ, Wilson CJ, and Paladini CA (2010). A dynamic role for GABA receptors on the firing pattern of midbrain dopaminergic neurons. J. Neurophysiol 104, 403–413. [PubMed: 20445035]

Lüscher C, Xia H, Beattie EC, Carroll RC, von Zastrow M, Malenka RC, and Nicoll RA (1999). Role of AMPA receptor cycling in synaptic transmission and plasticity. Neuron 24, 649–658. [PubMed: 10595516]

Author Manuscript Author Manuscript Author Manuscript Author Manuscript

Mendez JA, Bourque M-J, Fasano C, Kortleven C, and Trudeau L-E (2011). Somatodendritic dopamine release requires synaptotagmin 4 and 7 and the participation of voltage-gated calcium channels. J. Biol. Chem 286, 23928–23937. [PubMed: 21576241]

Mohebi A, Pettibone JR, Hamid AA, Wong JT, Vinson LT, Patriarchi T, Tian L, Kennedy RT, and Berke JD (2019). Dissociable dopamine dynamics for learning and motivation. Nature 570, 65–70. [PubMed: 31118513]

Montal M (2010). Botulinum neurotoxin: a marvel of protein design. Annu. Rev. Biochem 79, 591–617. [PubMed: 20233039]

Mozrzymas JW, Zarnowska ED, Pytel M, and Mercik K (2003). Modulation of GABA(A) receptors by hydrogen ions reveals synaptic GABA transient and a crucial role of the desensitization process. J. Neurosci 23, 7981–7992. [PubMed: 12954859]

Nirenberg MJ, Vaughan RA, Uhl GR, Kuhar MJ, and Pickel VM (1996a). The dopamine transporter is localized to dendritic and axonal plasma membranes of nigrostriatal dopaminergic neurons. J. Neurosci 16, 436–447. [PubMed: 8551328]

Nirenberg MJ, Chan J, Liu Y, Edwards RH, and Pickel VM (1996b). Ultrastructural localization of the vesicular monoamine transporter-2 in midbrain dopaminergic neurons: potential sites for somatodendritic storage and release of dopamine. J. Neurosci 16, 4135–4145. [PubMed: 8753875]

Nirenberg MJ, Chan J, Vaughan RA, Uhl GR, Kuhar MJ, and Pickel VM (1997). Immunogold localization of the dopamine transporter: an ultrastructural study of the rat ventral tegmental area. J. Neurosci 17, 5255–5262. [PubMed: 9204909]

Oswald MJ, Oorschot DE, Schulz JM, Lipski J, and Reynolds JNJ (2009). I_H current generates the afterhyperpolarisation following activation of subthreshold cortical synaptic inputs to striatal cholinergic interneurons. J. Physiol 587, 5879–5897. [PubMed: 19884321]

Overstreet LS, Westbrook GL, and Jones MV (2002). Measuring and modeling the spatiotemporal profile of GABA at the synapse. In Transmembrane Transporters, Quick WM, ed. (Wiley-Liss), pp. 259–275.

Patel JC, Witkovsky P, Avshalumov MV, and Rice ME (2009). Mobilization of calcium from intracellular stores facilitates somatodendritic dopamine release. J. Neurosci 29, 6568–6579. [PubMed: 19458227]

Petit-Jacques J, Sui JL, and Logothetis DE (1999). Synergistic activation of G protein-gated inwardly rectifying potassium channels by the βγ subunits of G proteins and Na^+ and Mg^{2+} ions. J. Gen. Physiol 114, 673–684. [PubMed: 10532964]

Philippart F, and Khaliq ZM (2018). Gi/o protein-coupled receptors in dopamine neurons inhibit the sodium leak channel NALCN. eLife 7, e40984. [PubMed: 30556810]

Planells-Cases R, Caprini M, Zhang J, Rockenstein EM, Rivera RR, Murre C, Masliah E, and Montal M (2000). Neuronal death and perinatal lethality in voltage-gated sodium channel α(II)-deficient mice. Biophys. J. 78, 2878–2891. [PubMed: 10827969]

Poulin J-F, Zou J, Drouin-Ouellet J, Kim K-YA, Cicchetti F, and Awatramani RB (2014). Defining midbrain dopaminergic neuron diversity by single-cell gene expression profiling. Cell Rep. 9, 930–943. [PubMed: 25437550]

Pucak ML, and Grace AA (1994). Evidence that systemically administered dopamine antagonists activate dopamine neuron firing primarily by blockade of somatodendritic autoreceptors. J. Pharmacol. Exp. Ther 271, 1181–1192. [PubMed: 7996424]

Puopolo M, Raviola E, and Bean BP (2007). Roles of subthreshold calcium current and sodium current in spontaneous firing of mouse midbrain dopamine neurons. J. Neurosci 27, 645–656. [PubMed: 17234596]

Rice ME, and Cragg SJ (2008). Dopamine spillover after quantal release: rethinking dopamine transmission in the nigrostriatal pathway. Brain Res. Brain Res. Rev 58, 303–313.

Rice ME, and Patel JC (2015). Somatodendritic dopamine release: recent mechanistic insights. Philos. Trans. R. Soc. Lond. B Biol. Sci 370, 1–14.

Robertson GS, Damsma G, and Fibiger HC (1991). Characterization of dopamine release in the substantia nigra by in vivo microdialysis in freely moving rats. J. Neurosci 11, 2209–2216. [PubMed: 1712381]

Author Manuscript Author Manuscript Author Manuscript Author Manuscript

Robinson BG, Bunzow JR, Grimm JB, Lavis LD, Dudman JT, Brown J, Neve KA, and Williams JT (2017). Desensitized D2 autoreceptors are resistant to trafficking. Sci. Rep 7, 4379. [PubMed: 28663556]

Santiago M, Machado A, and Cano J (1992). Fast sodium channel dependency of the somatodendritic release of dopamine in the rat's brain. Neurosci. Lett 148, 145–147. [PubMed: 1338647]

Stuhrman K, and Roseberry AG (2015). Neurotensin inhibits both dopamine- and GABA-mediated inhibition of ventral tegmental area dopamine neurons. J. Neurophysiol 114, 1734–1745. [PubMed: 26180119]

Sulzer D, Cragg SJ, and Rice ME (2016). Striatal dopamine neurotransmission: regulation of release and uptake. Basal Ganglia 6, 123–148. [PubMed: 27141430]

Takamori S, Holt M, Stenius K, Lemke EA, Grønborg M, Riedel D, Urlaub H, Schenck S, Brügger B, Ringler P, et al. (2006). Molecular anatomy of a trafficking organelle. Cell 127, 831–846. [PubMed: 17110340]

Wang W, Touhara KK, Weir K, Bean BP, and MacKinnon R (2016). Cooperative regulation by G proteins and Na+ of neuronal GIRK2 K+ channels. eLife 5, e15751. [PubMed: 27074662]

Wassef M, Berod A, and Sotelo C (1981). Dopaminergic dendrites in the pars reticulata of the rat substantia nigra and their striatal input. Combined immunocytochemical localization of tyrosine hydroxylase and anterograde degeneration. Neuroscience 6, 2125–2139. [PubMed: 6120482]

Wilson CJ, and Kawaguchi Y (1996). The origins of two-state spontaneous membrane potential fluctuations of neostriatal spiny neurons. J. Neurosci 16, 2397–2410. [PubMed: 8601819]

Witkovsky P, Patel JC, Lee CR, and Rice ME (2009). Immunocytochemical identification of proteins involved in dopamine release from the somatodendritic compartment of nigral dopaminergic neurons. Neuroscience 164, 488–496. [PubMed: 19682556]

Zhou F-W, Jin Y, Matta SG, Xu M, and Zhou F-M (2009). An ultra-short dopamine pathway regulates basal ganglia output. J. Neurosci 29, 10424–10435. [PubMed: 19692618]

Author Manuscript Author Manuscript Author Manuscript Author Manuscript

Highlights

- Somatodendritic DA release is decreased by single-cell Na^+-channel inhibition
- Intracellular BoNT/A LC cleaves SNAP-25 and eliminates DA release from the cell
- Synaptic GABA input to SNc DA neurons is unaffected by intracellular BoNT/A LC
- Somatodendritic DA in the SNc autoinhibits the neuron that releases it

Author Manuscript Author Manuscript Author Manuscript Author Manuscript

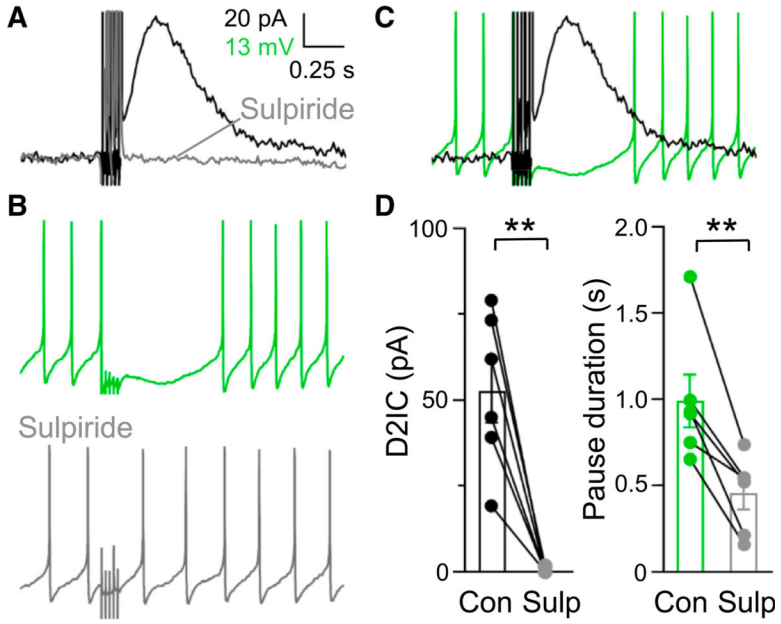

Figure 1. Electrical stimulation evokes a D2IC in SNc DA neurons that causes a pause in spontaneous activity

(A) Voltage-clamp record showing a D2IC evoked by local 5-pulse, 40-Hz stimulation before and after sulpiride (1 μM), a D2R antagonist.

(B) Example of spontaneous activity and a pause following 5-pulse, 40-Hz stimulation (top). The pause was abolished by sulpiride (bottom).

(C) Time course of evoked D2IC and pause in spontaneous activity in the SNc DA neuron in (A) and (B).

(D) Amplitude of evoked D2ICs and duration of D2-receptor-dependent pauses in spontaneous activity before and after sulpiride (Sulp) (control D2IC amplitude, 52.9 ± 8.4 pA; after sulpiride, 0.31 ± 0.26 pA, **$p < 0.01$; control pause duration, 0.99 ± 0.14 s; after sulpiride, 0.45 ± 0.08 s, **$p < 0.01$, $n = 6$; paired t test).

Author Manuscript Author Manuscript Author Manuscript Author Manuscript

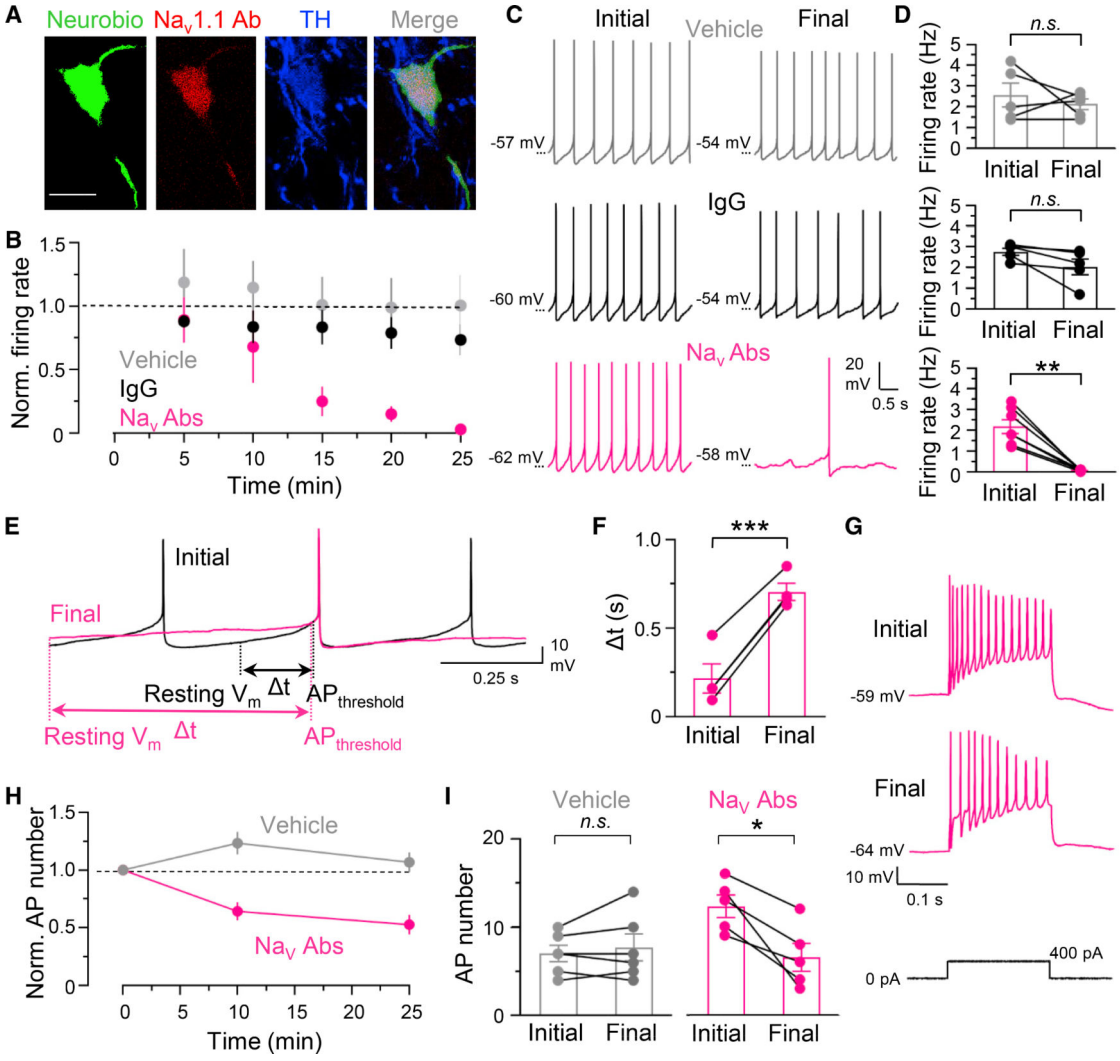

Figure 2. Single-cell application of Na_V Abs inhibits SNc DA neuron activity and decreases excitability

(A) $Na_V1.1$ Ab (secondary antibody only) and TH immunostaining in SNc after whole-cell recording; $Na_V1.2$ Ab immunostaining is illustrated in Figure S1B. Neurobiotin 488 was introduced with $Na_V1.1$ Ab via the recording pipette (n = 5 slices). Scale bar, 20 μm.

(B) Time course of spontaneous SNc DA neuron firing frequency over 25 min with intracellular application of vehicle (n = 5), IgG (n = 5), or $Na_V1.1$ Ab + $Na_V1.2$ Ab (Na_V Abs) (n = 7).

(C) Spontaneous activity with vehicle, IgG, or Na_V Abs in the pipette.

(D) Summary of Na_V Ab effects on spontaneous frequency (vehicle, 99% ± 23% of initial frequency, n = 5, p = 0.5; IgG, 79% ± 13%, n = 5, p = 0.15; $Na_V1.1$ Ab and $Na_V1.2$ Ab, 14% ± 5%, n = 7, **p < 0.01; paired t test).

(E) Spontaneous activity with Na_V Abs in the pipette; Δt is the time from resting membrane voltage (V_m) to AP threshold ($AP_{threshold}$).

(F) Quantification of Δt when recorded with Na_V Abs in the pipette (initial, 0.22 ± 0.07 s; final, 0.71 ± 0.04 s, ***p < 0.001). Bars are means ± SEM for n = 4; paired t test.

Author Manuscript Author Manuscript Author Manuscript Author Manuscript

(G) Response of SNc DA neurons recorded in current clamp during depolarizing current injection (+400 pA, 200 ms) after establishing whole-cell recording (initial) and the end of 25-min recording (final) with Na_v Abs in the pipette. Intracellular application of Na_v Abs decreased the number of APs evoked by current injection.

(H) Time course of the effect of single-cell application of Na_v Abs on AP number evoked during current injection (vehicle, n = 6; Na_v Abs, n = 5).

(I) AP number during current injection with vehicle or Na_v Abs in the pipette (vehicle, 106% ± 9% of initial, n = 6, p = 0.4; Na_v Abs, 64% ± 7%, n = 5, *p < 0.05; paired t test).

Author Manuscript Author Manuscript Author Manuscript Author Manuscript

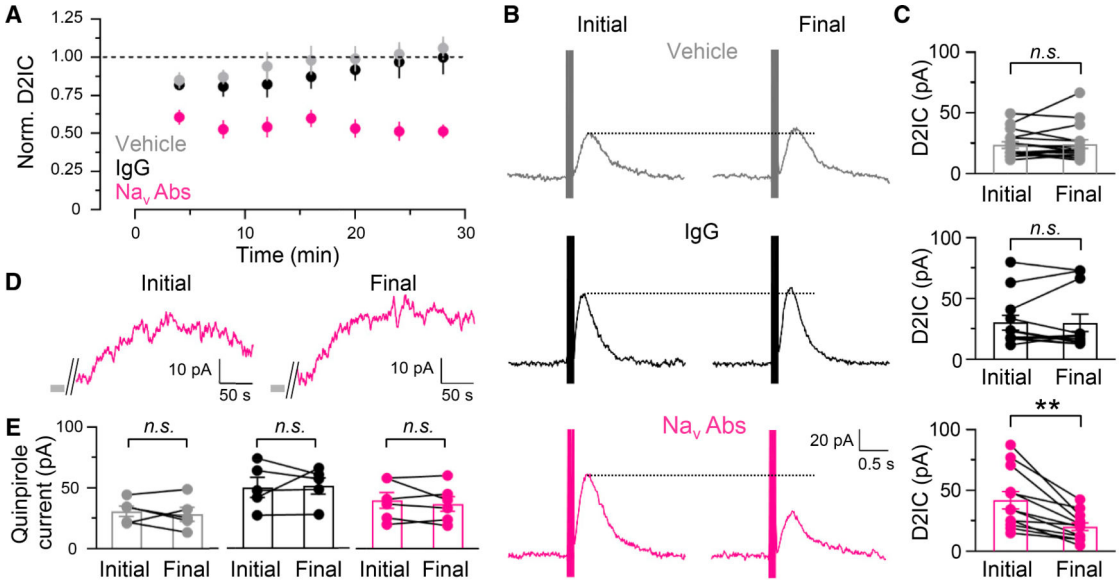

Figure 3. Single-cell application of Na_V Abs decreases evoked D2IC amplitude

(A) Average time course of changes in D2IC amplitude with vehicle (n = 16), IgG (n = 12), or $Na_V1.1$ Ab + $Na_V1.2$ Ab (Na_V Abs) (n = 12) in the recording pipette.

(B) D2ICs after establishing whole-cell recording (initial) and at the end of the recording period (final).

(C) Final D2IC amplitude recorded with vehicle, IgG, or Na_V Abs (vehicle, 104% ± 7% of initial, n = 16, p = 0.6; IgG, 98% ± 11%, n = 12, p = 0.6; pooled Na_V Abs, 51% ± 5%, n = 12, **p < 0.01; paired t test).

(D) Examples of D2 currents induced by brief superfusion of quinpirole (250 nM, 15 s). Quinpirole was applied immediately after establishing whole-cell recording (initial) and at the end (final) with Na_V Abs ($Na_V1.1$ + $Na_V1.2$ Abs or $Na_V1.1$ Ab) in the pipette. Gray bar indicates quinpirole duration.

(E) Quantification of quinpirole-evoked D2 currents with vehicle, IgG, or Na_V Abs (vehicle, 106% ± 16% of initial, n = 5, p = 0.6; IgG, 107% ± 11%, n = 5, p = 0.8; $Na_V1.1$ Ab and $Na_V1.2$ Ab [n = 4] or $Na_V1.1$ Ab [n = 2], 95% ± 8%, n = 6, p = 0.7; paired t test).

Author Manuscript Author Manuscript Author Manuscript Author Manuscript

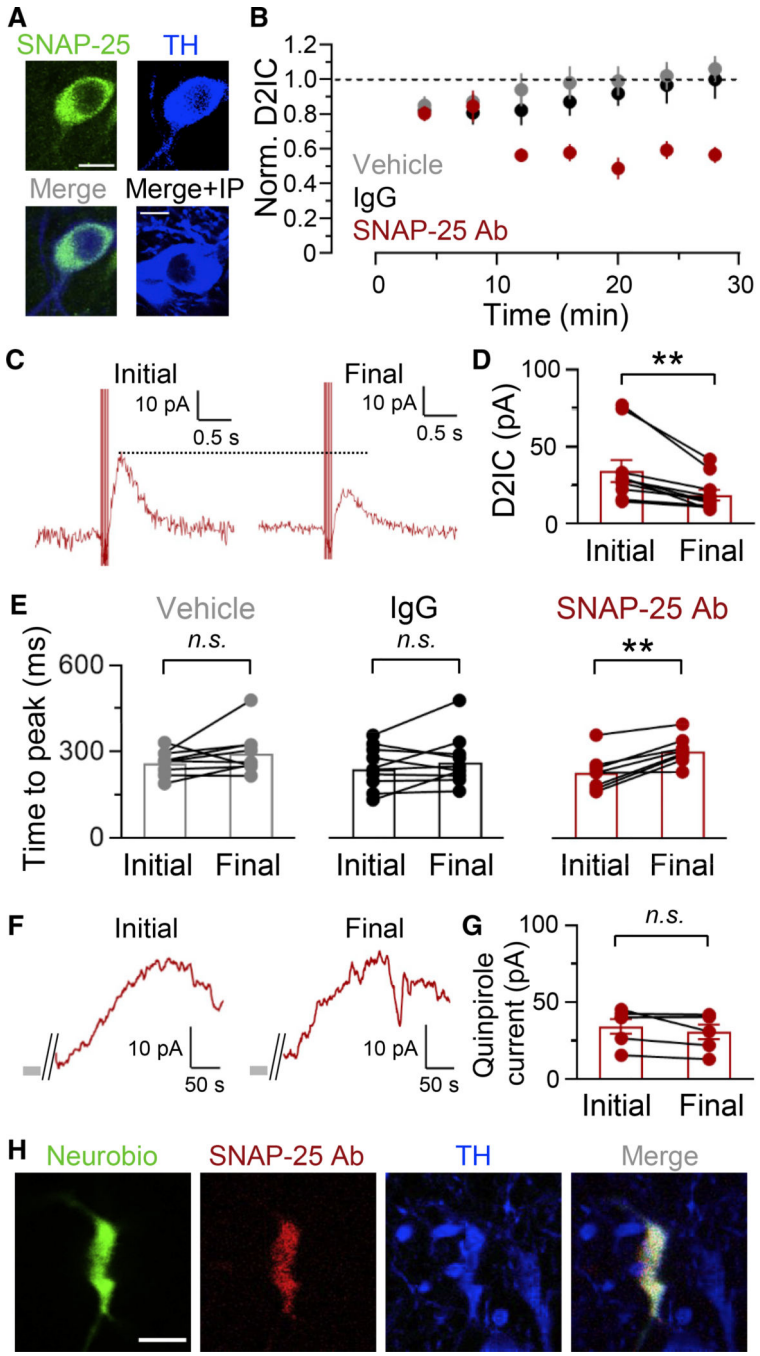

Figure 4. Intracellular application of SNAP-25 Ab decreases evoked D2IC amplitude

(A) SNAP-25-immunoreactivity (ir) and TH-ir in the SNc, demonstrating SNAP-25 in DA neurons (representative of sections from 18 mice). Pre-adsorption of SNAP-25 Ab with immunogenic peptide (IP) abolished ir (bottom right, sections from 2 mice). Scale bar, 10 μm.

(B) Average time course of changes in evoked D2IC amplitude recorded with single-cell application of SNAP-25 Ab via the pipette (vehicle, n = 16; IgG, n = 12; SNAP-25 Ab, n = 10).

Author Manuscript Author Manuscript Author Manuscript Author Manuscript

(C) Representative D2ICs immediately after establishing whole-cell recording (initial) and at the end of the recording period (final).
(D) Quantification of D2ICs in the presence of SNAP-25 Ab; mean D2IC amplitude with SNAP-25 Ab was 58% ± 4% of initial, n = 10, **p < 0.01; paired t test.
(E) Time to peak of D2ICs after establishing whole-cell recording and at the end of the recording period. Time to peak (vehicle, initial, 263 ± 13 ms; final, 296 ± 23 ms, n = 9, p = 0.2, IgG, initial, 245 ± 22 ms; final, 267 ± 26 ms, n = 10, p = 0.3, SNAP-25 Ab, initial, 229 ± 21 ms; final, 305 ± 16 ms, n = 8, **p < 0.01).
(F) Representative D2 currents evoked by brief superfusion of quinpirole (250 nM, 15 s). Quinpirole was applied at the beginning and end of recording with SNAP-25 Ab in the pipette. Gray bar indicates quinpirole duration.
(G) Quantification of final quinpirole-evoked D2 currents in the presence of SNAP-25 Ab (90% ± 5% of initial, n = 6, p = 0.2).
(H) Representative immunostaining for SNAP-25 Ab (secondary antibody only) and TH, with Neurobiotin 488 after whole-cell recording; Neurobiotin 488 was introduced with SNAP-25 Ab via the recording pipette (n = 2 slices for triple staining; n = 4 analyzed for Neurobiotin 488 and SNAP-25 Ab). Scale bar, 20 μm.

Author Manuscript Author Manuscript Author Manuscript Author Manuscript

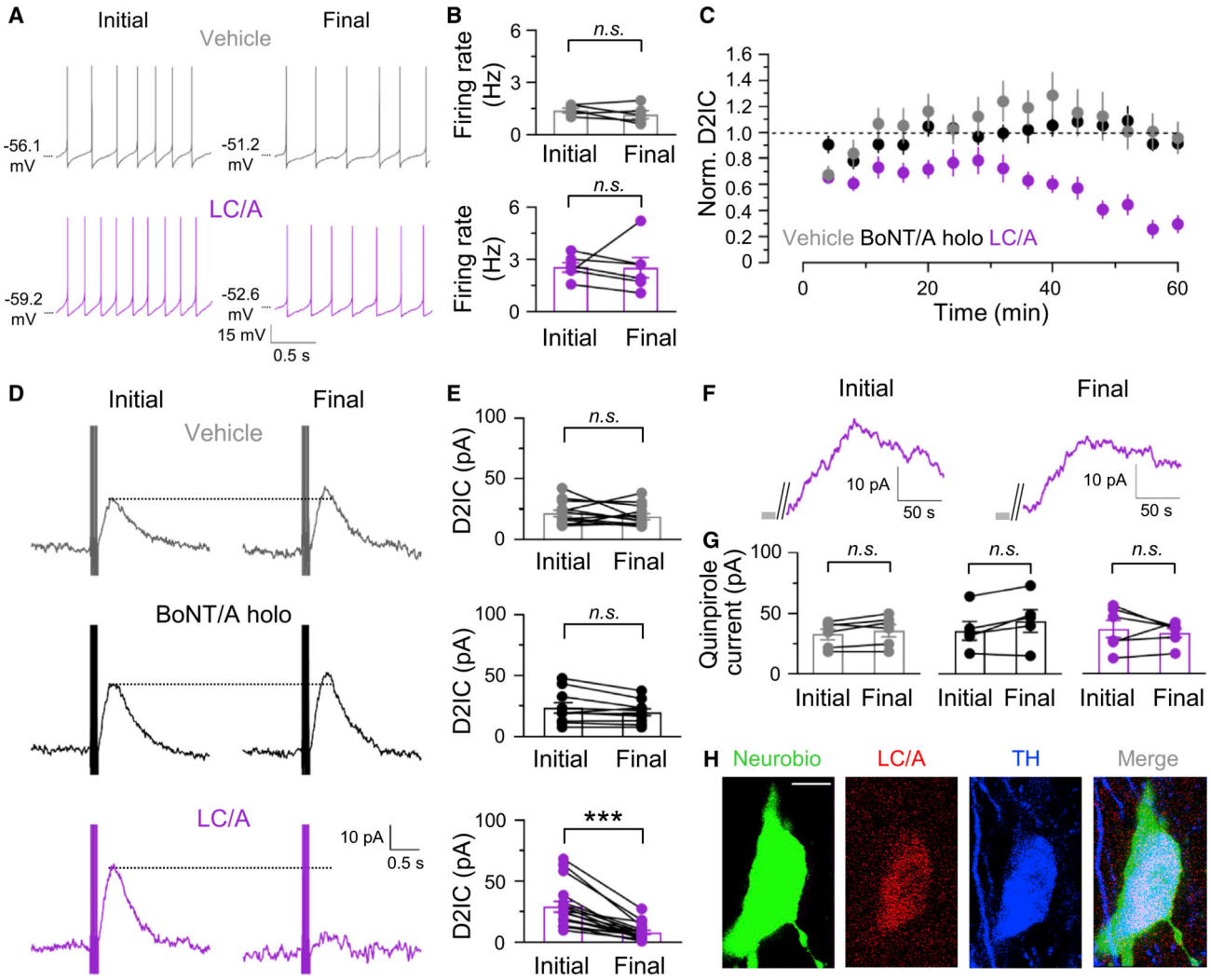

Figure 5. Single-cell application of LC/A decreases D2IC amplitude in SNc DA neurons without altering spontaneous activity

(A) Current-clamp records of spontaneous activity of SNc DA neurons with vehicle or LC/A in the pipette.

(B) Summary showing the lack of effect of LC/A in the pipette on SNc DA neuron pacemaker activity (vehicle, n = 5, p = 0.3; LC/A, n = 6, p = 0.9; paired t test).

(C) Average D2IC amplitude over time with vehicle (n = 12), BoNT/A holotoxin (holo) (n = 10), or LC/A (n = 17) in the pipette.

(D) Evoked D2IC after establishing whole-cell patch (initial) and at the end of the recording (final).

(E) Mean changes in D2IC amplitude recorded with vehicle, BoNT/A holo, or LC/A in the pipette (vehicle, 98% ± 13% of initial, n = 12, p = 0.4; BoNT/A holo, 90% ± 5%, n = 10, p = 0.07; LC/A, 34% ± 7%, n = 17 ***p < 0.001; paired t test).

(F) Quinpirole-evoked GIRK currents at the beginning and end of experiment. Gray bar indicates quinpirole duration.

Author Manuscript Author Manuscript Author Manuscript Author Manuscript

(G) Final quinpirole-evoked currents (quinpirole vehicle, 107% ± 4% of initial, n = 6, p = 0.14; BoNT/A holo, 121% ± 1%, n = 5, p = 0.06; LC/A, 104% ± 14%, n = 6, p = 0.5; paired t test).

(H) Representative immunostaining for LC/A and TH in the SNc after whole-cell recording with LC/A in the pipette; Neurobiotin 488 (Neurobio) was included in the pipette solution to mark recorded neurons (n = 5 slices). Scale bar, 10 μm.

Author Manuscript Author Manuscript Author Manuscript Author Manuscript

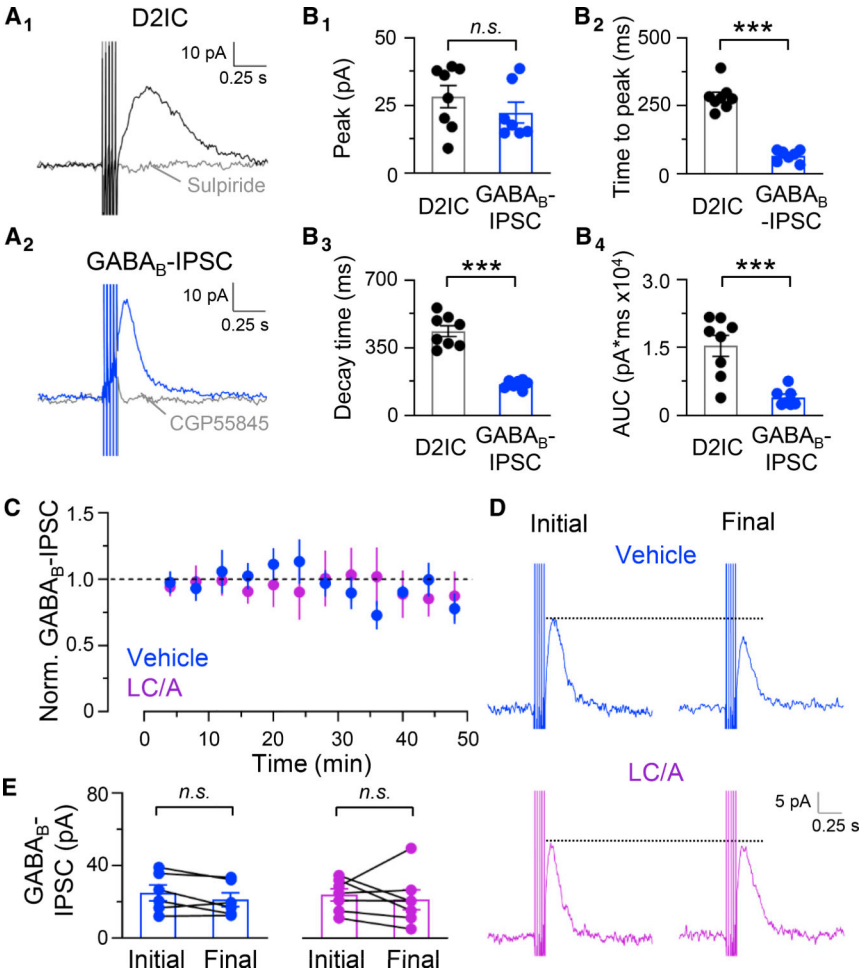

Figure 6. Distinct kinetics of D2ICs versus $GABA_B$ IPSCs in SNc DA neurons and lack of effect of LC/A on evoked $GABA_B$ IPSCs

(A) Evoked D2ICs and $GABA_B$ IPSCs recorded in separate DA neurons. Sulpiride (1 μM) abolished evoked D2ICs (A_1) and CGP55845 (300 nM), a $GABA_B$ receptor antagonist, abolished $GABA_B$ IPSCs (A_2).

(B) Kinetics of D2ICs and $GABA_B$ IPSCs. Comparison of peak amplitude (B_1), time to peak (B_2), decay time (B_3), and area under the curve (AUC) (B_4) for D2ICs (n = 8) and $GABA_B$ IPSCs (n = 7). Peak amplitude (D2IC, 28.3 ± 3.8 pA; $GABA_B$ IPSC, 22.3 ± 3.5 pA, p = 0.3), time to peak (D2ICs, 283 ± 16 ms; $GABA_B$ IPSCs, 66 ± 7 ms, ***p < 0.001), decay time constant (D2ICs, 436 ± 27 ms; $GABA_B$ IPSCs, 163 ± 9 ms, ***p < 0.001), AUC (pA*ms) (D2ICs, 15.4 ± 2.2 × 10^3; $GABA_B$ IPSC, 3.9 ± 0.7 × 10^3, ***p < 0.001). Bars are means ± SEM; unpaired t test.

(C) Time course of evoked $GABA_B$ IPSC amplitude, normalized to initial for each DA neuron with vehicle or LC/A in the pipette (vehicle, n = 6; LC/A, n = 7).

(D) Representative evoked $GABA_B$ IPSC recorded in voltage-clamp mode after establishing whole-cell recording (initial) and at the end of recording (final).

(E) Final $GABA_B$ IPSCs recorded with vehicle or LC/A (vehicle, 88% ± 9% of initial, n = 6, p = 0.12; LC/A, 86% ± 16%, n = 7, p = 0.5; paired t test).

Author Manuscript Author Manuscript Author Manuscript Author Manuscript

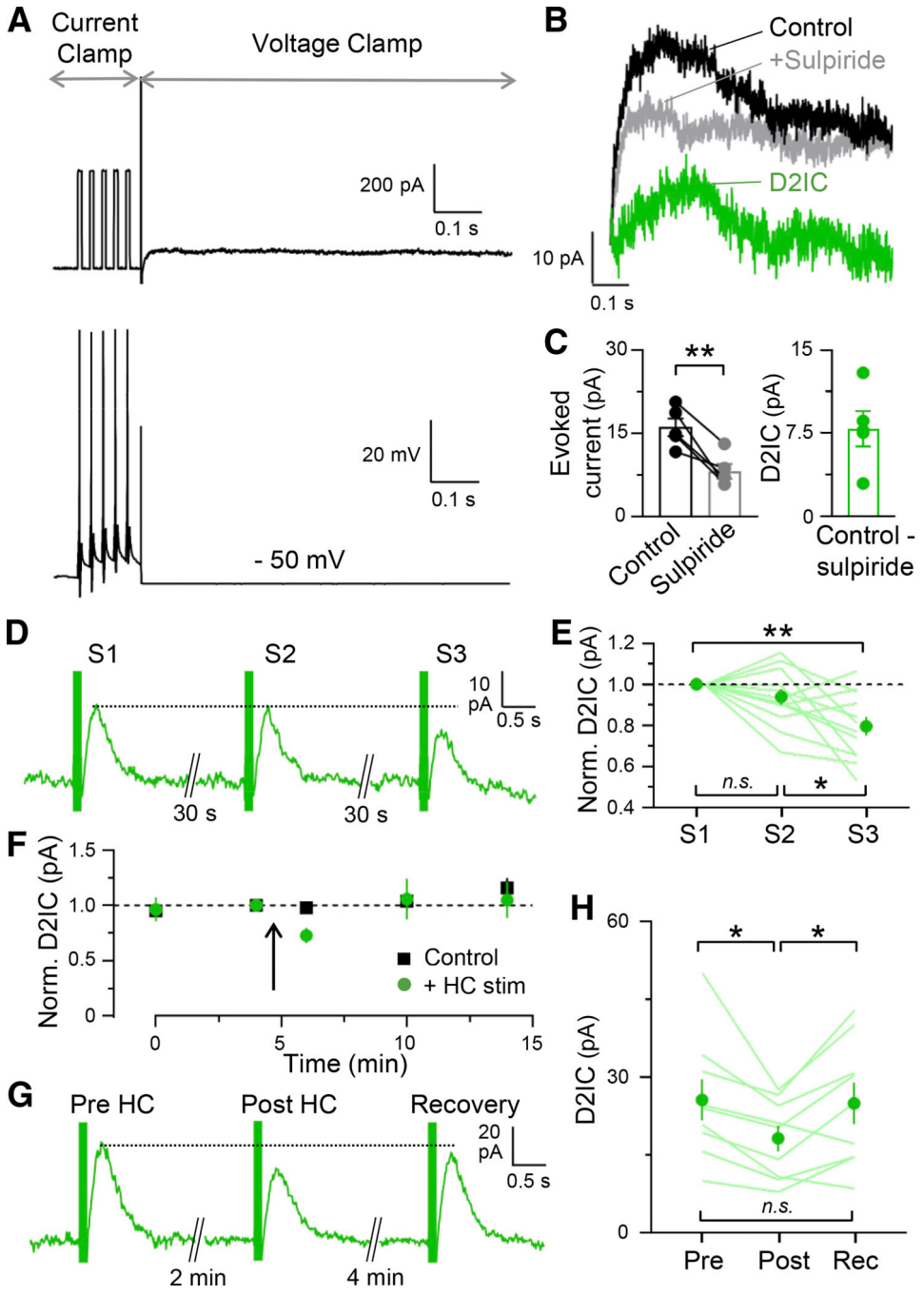

Figure 7. Evoked D2ICs in individual SNc DA neurons using HC

(A) Schematic of HC protocol with current (top) and voltage traces (bottom). An SNc DA neuron was stimulated in current clamp by five current pulses (400 pA, 8-ms duration) at 40 Hz, followed by a switch to voltage clamp at −50 mV to record the resulting current.

(B) Averaged current responses of SNc DA neurons (n = 5) recorded when the holding potential was returned to −50 mV after current-clamp stimulation and before and after sulpiride (1 μM). The D2IC trace is the average of the difference between control and sulpiride for each SNc DA neuron.

Author Manuscript Author Manuscript Author Manuscript Author Manuscript

(C) Evoked current before and after sulpiride (1 μM), with D2IC amplitude calculated as control minus sulpiride (control, 16.1 ± 1.4 pA; after sulpiride, 8.1 ± 1.2 pA, n = 5, **p < 0.01, paired t test; D2IC, 8.0 ± 1.4 pA).

(D) Use-dependent depression of evoked D2ICs with repeated local stimulation (5 pulse, 40 Hz). Three stimulations were delivered at 30-s intervals (S1–S3).

(E) Quantification of D2IC depression (40 Hz, 5 pulses) (S2, 94% ± 4% of S1; 3S, 80% ± 5% of S1, n = 12, **p < 0.01 S1 versus S3, *p < 0.05 S2 versus S3; one-way ANOVA, Tukey post hoc test).

(F) Amplitude of locally evoked D2ICs without (Control) and with preceding HC stimulation. After establishment of stable D2ICs at 4-min intervals, the HC stimulation protocol was initiated (arrow): 40 Hz, 5 pulses (400 pA, 8 ms duration) applied three times at 30-s intervals, followed by a 4-min interval before local stimulation to assess recovery (Control, post HC time point, 98% ± 3% of pre, p = 0.9, n = 5, recovery time point, 113% ± 8% of pre, p = 0.4, n = 5; one-way ANOVA, Tukey post hoc test).

(G) D2ICs evoked by local stimulation at pre-HC, post-HC, and recovery.

(H) Amplitude of locally evoked D2ICs at pre-HC, post-HC, and recovery (post-HC, 72% ± 6% of pre, recovery HC, 102% ± 11% of pre, n = 9, *p < 0.05 for pre- versus post-HC, post versus recovery HC; one-way ANOVA, Tukey post hoc test).

Author Manuscript Author Manuscript Author Manuscript Author Manuscript

KEY RESOURCES TABLE

REAGENT or RESOURCE	SOURCE	IDENTIFIER
Antibodies		
anti-SNAP-25 rabbit polyclonal	Synaptic Systems	Cat# 111 002; RRID:AB_887790
anti-$Na_v1.1$ rabbit polyclonal	Alomone Labs	Cat# ASC-001; RRID:AB_2040003
anti-$Na_v1.2$ rabbit polyclonal	Alomone Labs	Cat# ASC-002; RRID:AB_2040005
IgG rabbit polyclonal	Abcam	Cat# ab176094; RRID:N/A
anti-Tyrosine hydroxylase sheep polyclonal	Abcam	Cat# ab113; RRID:AB_297905
anti-sheep Cy5	Jackson ImmunoResearch Labs	Cat# 713–175–147; RRID:AB_2340730
anti-rabbit Cy3	Jackson ImmunoResearch Labs	Cat# 711–225–152; RRID:AB_2340612
anti-human Cy3	Jackson ImmunoResearch Labs	Cat# 709–225–149; RRID:AB_2340541
Neurobiotin 488	Vector Labs	Cat# SP-1125; RRID:AB_2336605
anti-botulinum toxin A light chain human monoclonal	Laboratory of Dr. James D. Marks, UCSF	N/A
Chemicals, peptides, and recombinant proteins		
(S)-sulpiride	Sigma-Aldrich	Cat # S7771
picrotoxin	Sigma-Aldrich	Cat # A1675
CGP55845 hydrochloride	Tocris	Cat # 1428
(-)-quinpirole hydrochloride	Tocris	Cat # 1061
D-AP5	Tocris	Cat # 0106
DNQX	Tocris	Cat # 0189
QX314	Sigma-Aldrich	Cat # L5783
YM298198 hydrochloride	Hello Bio	Cat # HB0664
LC/A	Laboratory of Dr. Konstantin Ichtchenko, NYU	N/A
BoNT/A holotoxin	Metabiologics	Cat# BoNT/A isolated toxin
Experimental models: Organisms/strains		
Mouse: C57B6J	Jackson Laboratory	JAX: 000664; RRID:IMSR_JAX:000664
Software and algorithms		
Graphpad Prism 8	Graphpad Software	https://www.graphpad.com/; RRID: SCR_002798
ImageJ	NIH	https://imagej.nih.gov/ij/; RRID: SCR_003070
Adobe Photoshop CC2015	Adobe Systems	https://www.adobe.com/; RRID: SCR_014199
pClamp 10	Molecular Devices	https://mdc.custhelp.com/; RRID: SCR_011323